024562-2-F

THEORETICAL CHARACTERIZATION OF MICROSTRIP LUMPED ELEMENTS AND INTERCONNECTS IN $M^3IC'S$

by

P.B. Katehi
D. Pavlidis

Department of Electrical Engineering and Computer Science
The University of Michigan
Ann Arbor, MI 48109-2122

PROGRESS REPORT

1. **ARO Proposal Number:** 23836-EL

2. **Period Covered By Report:** 1 January 1989- 30 June 1989

3. **Title of the Proposal:** Theoretical and Experimental Study of Microstrip Discontinuities in Millimeter Wave Integrated Circuits.

4. **Contract Number:** DAAL03-87-K-0088

5. **Name of Institution:** University of Michigan

6. **Authors of Report:** Pisti B. Katehi
Dimitris Pavlidis

7. **Listings of Interim Reports and Manuscripts Submitted or Published Under Full or Partial ARO Sponsorship During This Reporting Period:**

1) T.E. Van Deventer, P.B. Katehi and A.C. Cangellaris, "High Frequency Conductor and Dielectric Losses in Shielded Microstrip", 1989 IEEE MTT-S International Microwave Symposium Digest, Vol. III, pp. 919-922 (Appendix A).

2) W.P. Harokopus and P.B. Katehi, "Analysis of Multilayer Irregular Microstrip Discontinuities Including Radiation Losses". To appear in the Proceedings of the 19th European Microwave Conference, London, England, September 1989 (Appendix B).

3) W.P. Harokopus and P.B. Katehi, "Characterization of Microstrip Discontinuities on Multilayer Dielectric Substrates Including Radiation Losses". Accepted for publication in the IEEE Trans. on Microwave Theory and Techniques, December 1989 (Appendix C)

4) T.E. van Deventer, P.B. Katehi and A.C. Cangellaris, "An Integral Equation Method for the Evaluation of Conductor and Dielectric Losses in High Frequency Interconnects". Accepted for publication in the IEEE Trans. on Microwave Theory and Techniques, December 1989 (Appendix D)

8. Scientific Personnel Supported By This Project:

Faculty	Graduate Students
P.B. Katehi	E.T. van Deventer
D. Pavlidis	W.P. Harokopus
	Research Engineer
	M. Weiss

RESEARCH TASKS

Title	Personel Involved with the Research
1. High Frequency Conductor and Dielectric Losses in Micro-Strip Interconnects.	P.B. Katehi T.E. van Deventer
2. Characterization of High Frequency Superconducting Lines	P.B. Katehi T.E. van Deventer
3. Radiation Losses in Antenna Feeding Networks.	P.B. Katehi W.P. Harokopus
4. Characterization of Microstrip Lumped Elements	P.B. Katehi W.P. Harokopus
5. Gate Capacitance Modeling of GaAs MESFET's in Millimeter Wave Frequencies.	D. Pavlidis M.Weiss P.B. Katehi

1. HIGH FREQUENCY CONDUCTOR AND DIELECTRIC LOSSES IN MICROSTRIP INTERCONNECTS.

Faculty Supervisor: Pisti B. Katehi

Graduate Student Participant: T.E. van Deventer

Period: 1 January 1989 - 30 June 1989.

Work Performed:

An integral equation method has been developed to solve for th complex propagation constant in multi-layered planar structures wit arbitrary number of strip conductors on different levels. The Green's function included in the integral equation has been derive by using a generalized impedance boundary formulation. The microstrip ohmic losses have been evaluated by using an equivalent frequency-dependent impedance surface which is derived by solving for the fields inside the conductors. This impedance surface replaces the conducting strips and takes into account the thickness and skin effect of the strips at high frequencies.

Using the above described procedure, results have been generated for single microstrip lines on one and two-level multipl interconnects. Also, the effects of various parameters such as frequency, thickness of the lines and substrate surface roughness the complex propagation constant are investigated. Results derive from this analysis show very good agreement with available literature data.

Program for Next Period:

During the next period, this method will be extended to characterize three dimensional structures such as two-level interconnects crossing at arbitrary angles. Also, using this analysis, the effect of conductor losses on high frequency

directional couplers and lumped elements will be studied and design curves will be generated.

Publications and Reports:

T.E. Van Deventer, P.B. Katehi and A.C. Cangellaris, "High Frequency Conductor and Dielectric Losses in Shielded Microstrip", 1989 IEEE MTT-S International Microwave Symposium Digest, Vol. III, pp. 919-922 (Appendix A).

T.E. van Deventer, P.B. Katehi and A.C. Cangellaris, "An Integral Equation Method for the Evaluation of Conductor and Dielectric Losses in High Frequency Interconnects". Accepted for publication in the IEEE Trans. on Microwave Theory and Techniques, December 1989 (Appendix D).

2. CHARACTERIZATION OF HIGH FREQUENCY SUPERCONDUCTING LINE

Faculty Supervisor: Pisti B. Katehi

Graduate Student Participant: T.E. van Deventer

Period: 1 June 1989 - 30 June 1989

Work Performed:

This project started recently in cooperation with the Hughes Research Laboratories at Malibu, California. The purpose of this work is the accurate high frequency theoretical and experimental characterization of High Tc superconducting lines , filters, resonators e.t.c. The analysis is based on an integral equation approach similar to the one described in task 1. The theoretical results will be verified by comparing to experimental data which a to be obtained at Hughes Malibu.

At the present time, we derive theoretical data for single a coupled superconducting lines.

Program for Next Period:

During the next period, a program will be developed to solve three-dimensional structures such as filters and resonators. Also, the same circuits will be measured and the experimental results wi be compared to theoretical ones for code validation.

3. RADIATION LOSSES IN ANTENNA FEEDING NETWORKS.

Faculty Supervisor: Pisti B. Katehi

Graduate Student Participant: W.P. Harokopus

Period: 1 January 1989 - 30 June 1989

Work Performed:

Antenna feeding networks consist of sections of lines connected to each other through junctions or terminated to various distributed resistive or reactive loads. All these discontinuities and lumped elements radiate resulting in higher losses and stronger coupling to neighboring radiating structures. The losses and the coupling are the main contributors to antenna gain and efficiency reduction. In order to be able to improve the array performance the understanding of the power loss mechanisms in array's feeding networks is very important especially at higher frequencies.

During the last six months, a full electromagnetic analysis of open microstrip discontinuities on multilayered dielectric substrates has been presented. The space domain method of moments formulation accounts fully for all electromagnetic coupling, and space and surface wave radiation. Results for various multilayer discontinuities such as microstrip bends have been derived and the radiation properties have been studied.

Program for Next Period:

The radiation properties of geometricaly more complicated circuit elements will be studied extensively. Also, the surface wave and space wave patterns for the above circuit elements will be computed and measured. The measurements will be conducted at the facilities of the radiation laboratory at the University of Michigan

Publications and Reports:

W.P. Harokopus and P.B. Katehi, "Analysis of Multilayer Irregular Microstrip Discontinuities Including Radiation Losses". To appear i the Proceedings of the 19th European Microwave Conference, London, England, September 1989 (Appendix B)

W.P. Harokopus and P.B. Katehi, "Characterization of Microstrip Discontinuities on Multilayer Dielectric Substrates Including Radiation Losses". Accepted for publication in the IEEE Trans. on Microwave Theory and Techniques, December 1989 (Appendix C)

4.Characterization of Microstrip Lumped Elements.

Faculty Supervisor: Pisti B. Katehi

Graduate Student Participant: W.P. Harokopus

Period: 1 January 1989 - 30 June 1989

Work Performed:

Using the integral equation method which is presented in [2](Appendix B) preliminary results have been derived for the case of a multilevel spiral inductor and a meander line. The derived data are in the form of frequency dependent scattering parameters. At the present time, we perform an extensive analysis of the high frequency behavior of these elements and their radiation properties.

Program for Next Period:

During the next period, extensive numerical data will be derived for the case of spiral inductors, meander lines and overlay capacitors. In addition, the already developed codes will be modified to take into account conductor and dielectric losses.

5. GATE CAPACITANCE MODELING OF GaAs MESFETS's IN MILLIMETE WAVE FREQUENCIES.

Faculty Supervisor: D. Pavlidis
P.B. Katehi

Graduate Student Participant: I.S.Nikolaou
M. Weiss

Period: 1 January 1989 - 30 June 1989

Work Performed:

In the last semi-annual report (January 1989), a brief description of the method applied for the high-frequency modeling of the Gate in a MESFET was given. During the last six months, a FORTRAN program based on that method has been developed. At the present time, we try to verify its accuracy by comparing to existing data for simple structures such as a single microstrip line.

Program for Next Period:

During the next six months, we will derive data for more complicated structures such as a Field-Effect-Transistor. The derived results will be in the form of frequency-dependent gate-to drain and gate-to-source capacitances

HIGH FREQUENCY CONDUCTOR AND DIELECTRIC LOSSES IN SHIELDED MICROSTRIP

T.E. van Deventer*, P.B. Katehi* and A.C. Cangellaris**

*Radiation Laboratory, University of Michigan, Ann Arbor, MI
**Electrical and Computer Engineering Department, University of Arizona, Tucson, AZ

Abstract-

An integral equation method is developed to calculate the dispersion of non-perfectly conducting microstrip lines. Both dielectric losses in the substrate and conductor losses in the strips and ground plane are considered. Multiple conductors on several layers can be studied using an impedance boundary formulation for the derivation of the Green's function. The microstrip losses are evaluated by using a frequency-dependent surface impedance which is derived by solving the fields in the conductors. This surface impedance replaces the conducting strip and takes into account the thickness and skin effect of the strip at high frequencies. Good agreement with available literature data is shown.

INTRODUCTION

The effect of conductor losses in microstrip circuits and especially MMIC's is important to the circuit designer who is concerned with dissipation and power loss. Several studies have been performed to calculate the dispersion in microstrip structures at microwave frequencies considering dielectric and conductor losses. Conductor losses have first been analyzed by Wheeler [1] and Pucel [2] where a technique based on the *incremental-inductance rule* was used. Other approaches to the problem of losses include quasi-TEM models and the conventional perturbation technique as in [3] using a spectral-domain approach. However, these methods are limited to the case where the thickness of the strip is much larger than the skin depth. In the present study, a method is applied that represents conductor losses in microstrip lines by using a frequency-dependent impedance boundary, thus taking into account the skin-effect problem. The procedure applied for the solution of this problem is very powerful and general. In fact it can be applied to any number of problems including thin metallizations. The proposed method will be applied to

various interconnects and their propagation characteristics will be studied in the presence of other lines or under the effect of the shielding cavity.

THEORETICAL DERIVATION

Shielded planar microstrip transmission lines inside an inhomogeneously filled waveguide are considered as shown in Figure 1. Both dielectric losses in the substrate and conductor losses in the strip and ground plane are accounted for. The side walls are assumed perfect conductors. Because of the shielded structure, these lines propagate hybrid modes which have non-zero cut-off frequencies with the exception of the dominant mode. The LSE and LSM modes propagating along the z-direction can be obtained by solving the related boundary value problem.

The dyadic Green's function for the problem is derived in the spectral domain using the boundary conditions on the perfectly conducting walls and an equivalent impedance boundary condition on the interfaces. The current has a transverse component and a longitudinal component. Their variation in the y-direction is chosen such that the edge conditions on the strips are satisfied. The electric field is then given by Pocklington's integral equation as

$$\bar{E}(x = x') = \int\int \bar{\bar{\Gamma}}(x/x') \,.\, \bar{J}(y')\, e^{-jk_z^{MS}z'}\, dy'\, dz', \tag{1}$$

where k_z^{MS} is the unknown complex propagation constant of the microstrip. The Fourier transform used is given by

$$\bar{\bar{\Gamma}} \;=\; \frac{1}{2\pi}\int_{-\infty}^{\infty} \tilde{\bar{\bar{\Gamma}}}\, e^{-jk_z z}\, dk_z. \tag{2}$$

Substituting (2) in (1) and using the sifting property of the Fourier transform, the electric field becomes

$$\bar{E}(x = x') = \int \tilde{\bar{\bar{\Gamma}}}(x/x') \,.\, \bar{J}\, dy' \;|_{k_z = k_z^{MS}}. \tag{3}$$

One more condition needs to be applied, i.e. the boundary condition on the microstrip. For perfect conductors, the tangential electric field vanishes on the line. In this study, we approximate the strip with an equivalent non-zero frequency-dependent surface impedance boundary extending over the surface of the strip. It is desirable that this surface impedance describes, in a physical equivalent sense, the frequency-dependent field penetration in the lossy strips. In [5],[6] an integral equation formulation was presented for the evaluation of the frequency-dependent longitudinal current distribution in rectangular microstrip lines. This method allows us to compute the per unit length resistance $R(f)$ and the per unit length

internal inductance of the strip $L_{in}(f)$ as function of frequency. An equivalent longitudinal surface impedance can be defined then as

$$Z_l(f) \equiv \frac{E_z}{H_y} = (R(f) + j\,2\pi f\,L_{in})w, \tag{4}$$

where w is the width of the strip. As far as the transverse component of the current is concerned, the standard surface impedance for an infinite resistive plane is used,

$$-\frac{E_y}{H_z} \equiv Z_s(f) = (1+j)\frac{1}{\sigma\delta}, \tag{5}$$

where σ is the conductivity of the strip and δ the skin depth at the frequency of interest. Despite the fact that the width of the strip is finite, use of (5) is justified by the fact that the strip is assumed to be infinite in the direction perpendicular to the flow of the transverse component of the current. In addition, for most practical purposes, $|J_y| \ll |J_z|$, therefore the dominant part of the conductor loss is due to the longitudinal component of the current, for which the more accurate longitudinal surface impedance $Z_l(f)$ has been proposed. The boundary condition for the magnetic field on the surface impedance boundary gives

$$\hat{n} \times \bar{H} = \bar{J}. \tag{6}$$

In view of (4-6), (3) becomes

$$\int \{\,\tilde{\bar{\bar{\Gamma}}}(x/x') \,.\, \bar{J}\,dy' \;-\; Z_{l,s}\,\bar{J}\,\}\,|_{k_z=k_z^{Ms}} = 0 \tag{7}$$

which is the pertinent integral equation for the problem. The formulation of the Green's function results in a simple expression involving a single summation over the modes in the y-direction. The resulting homogeneous equation is solved for the microstrip propagation constant at the plane $z = 0$ with as many as a thousand modes to insure convergence. The method of moments is applied using a variation of Galerkin's procedure. Entire domain functions are used to solve for the current distribution. The above expression can be easily programmed on a personal computer to evaluate the propagation constant of the dominant and higher order microstrip modes.

RESULTS

The objective of this study is to determine the dispersion characteristics of single and multiple microstrip lines on single and multilayered substrates. Based on the theory derived in the previous section, a computer program has been developed to calculate the complex zeros of an analytic complex function using the Muller's algorithm with deflation.

Results on attenuation due to lossy dielectrics compare very well with available data. When considering conductor losses, the normalized phase constant of the dominant mode is seen to be slightly larger when no substrate losses are considered (see Figure 2). As the loss tangent of the substrate increases, the phase constant is smaller than in the case of a perfect conductor. As frequency increases, the phase constant tends toward the perfect conductor case. The attenuation constant of the dominant mode increases as expected when including conductor losses (see Figure 3). Attenuation for the case of a single strip and coupled strips is shown in Figures 4 and 5 respectively. Results are compared to the perturbational approach used in the spectral domain [3],[4] and in the finite-element method [7] . The method presented in this paper will be implemented to evaluate high frequencies dielectric and conductor losses for various interconnects and results will be presented.

CONCLUSIONS

An integral equation approach is applied to calculate the propagation constant of multiple strips on multilayered substrates. An equivalent impedance boundary is employed that takes into account the finite conductivity of the strips and extends to the case where the thickness of the conductor is of the same order of magnitude as the skin depth. Phase constant and attenuation for single and coupled strips are presented.

ACKNOWLEDGMENTS

This work was supported by the Army Research Office under contract project DAAL03-K-0088(23836-EL).

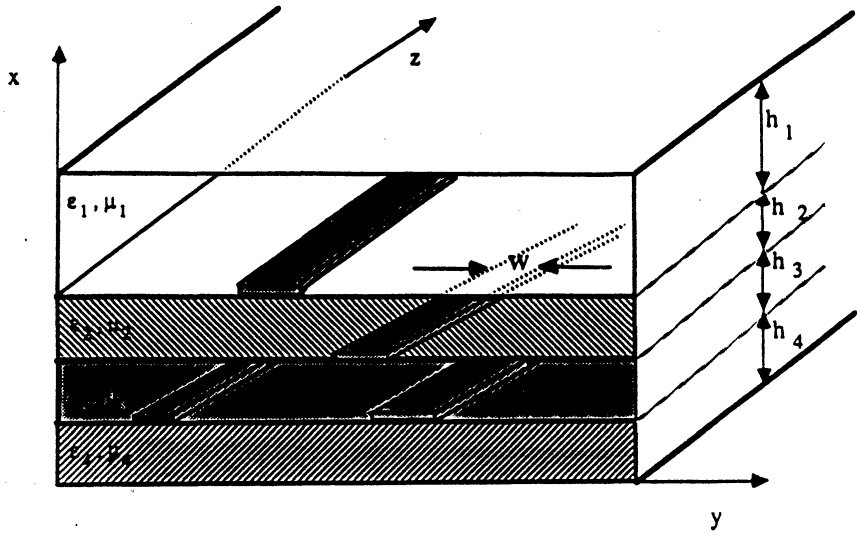

Figure 1: Shielded microstrip line configuration

References

[1] H. A. Wheeler, "Formulas for the Skin Effect," *Proc. IRE*, vol. 30, pp 412-424, Sept. 1942.

[2] R. A. Pucel, D. J. Masse, C. P. Hartwig, "Losses in Microstrip," *IEEE Trans. Microwave Theory Tech.*, vol. MTT-16, p 342, June 1968.

[3] D. Mirshekar-Syahkal, J. B. Davies, "Accurate Solution of Microstrip and Coplanar Structures for Dispersion and for Dielectric and Conductor Losses", *IEEE Trans. Microwave Theory Tech.*, vol. MTT-27, No. 7, pp 694-699, July 1979.

[4] D. Mirshekar-Syahkal, "An Accurate Determination of Dielectric Loss Effect in Monolithic Microwave Integrated Circuits Including Microstrip and Coupled Microstrip Lines," *IEEE Trans. Microwave Theory Tech.*, vol. MTT-31, No. 11, pp 950-954, November 1983.

[5] A.C. Cangellaris, "The importance of skin-effect in microstrip lines at high frequencies", *IEEE MTT-International Symposium Digest*, pp 197-198, May 1988.

[6] A.C. Cangellaris et al., "Real Inductance Calculation for High Speed Interconnect Systems," *International Electronic Packaging Conference*, Dallas, Texas, November 1988.

[7] Z. Pantic-Tanner, R. Mittra, "Finite-Element Matrices for Loss Calculation in Quasi-TEM Analysis of Microwave Transmission Lines," *Microwave and Optical Technology Letters*, vol. 1, No. 4, pp 142-146, June 1988.

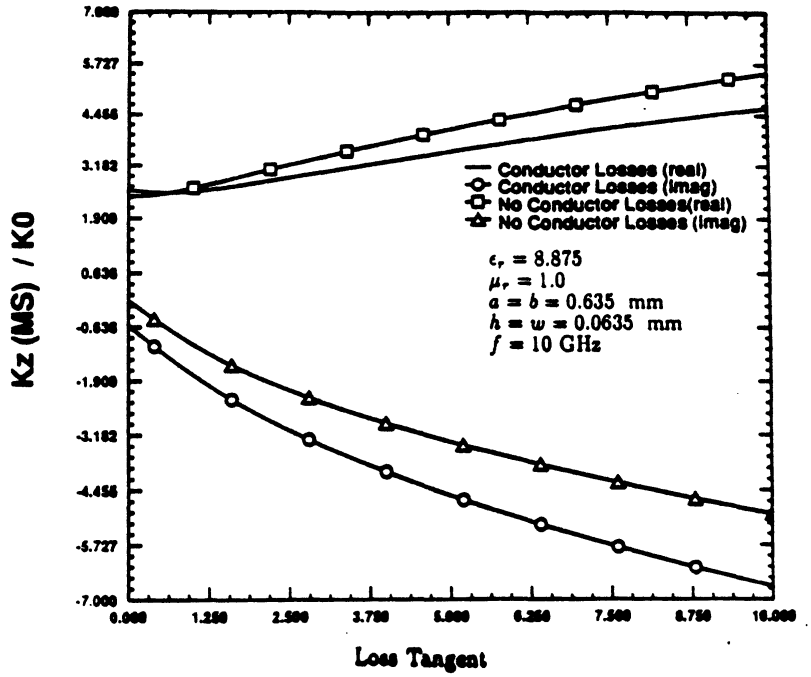

a. Propagation constant vs. loss tangent at $f = 10$ GHz

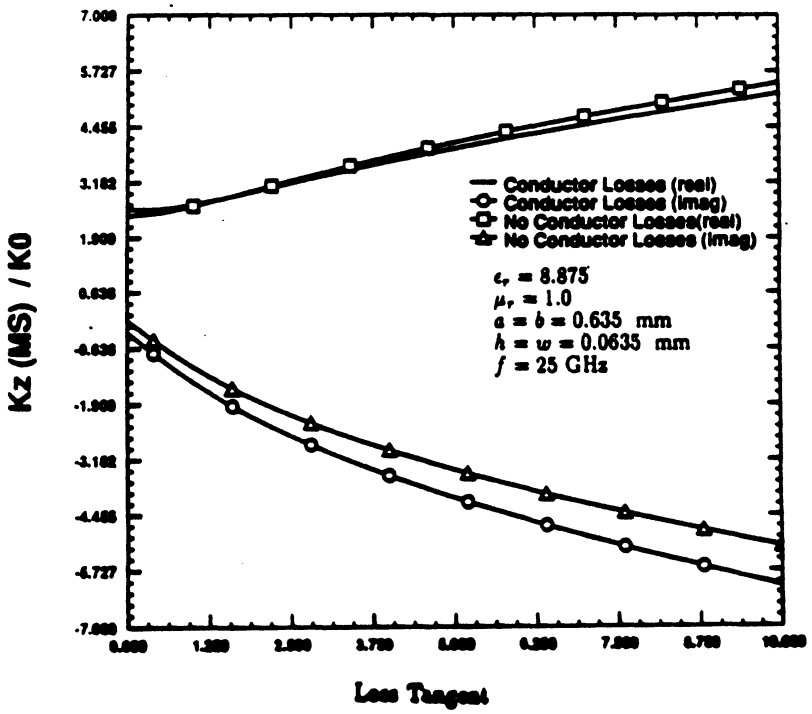

b. Propagation constant vs. loss tangent at $f = 25$ GHz

Figure 2: Effect of conductor losses on propagation constant of the dominant microstrip mod as a function of loss tangent

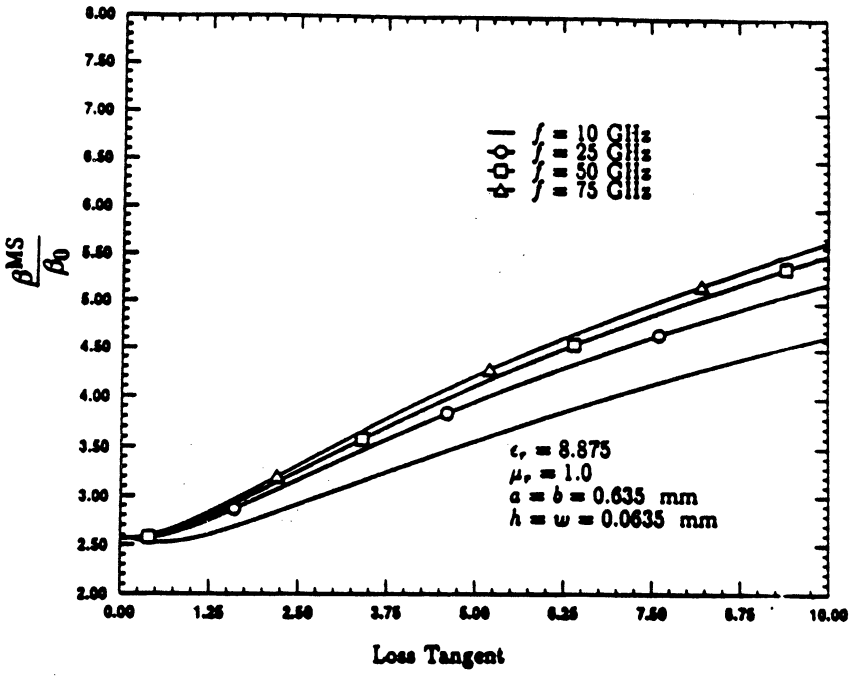

a. Phase constant as a function of substrate loss tangent

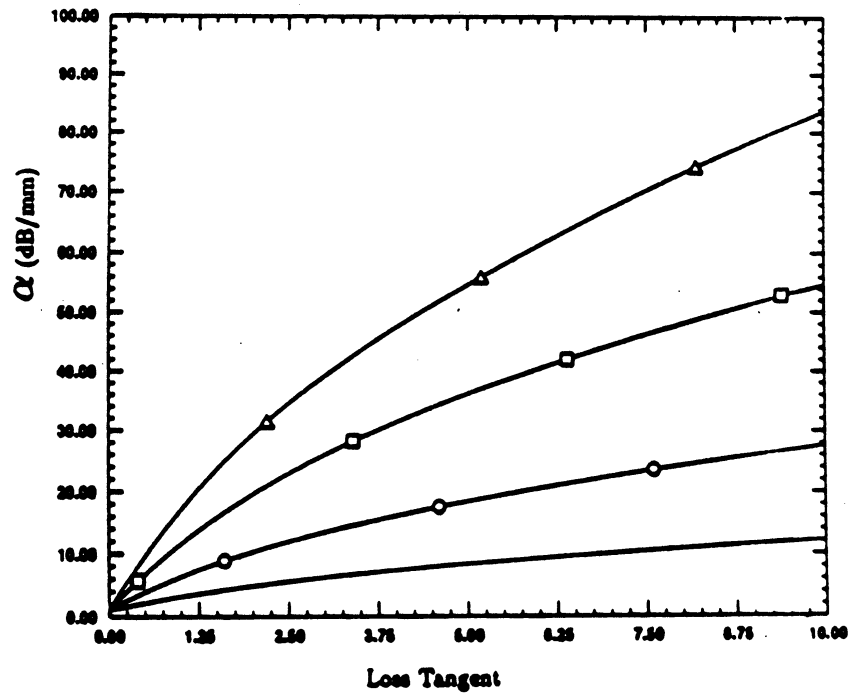

b. Attenuation constant as a function of substrate loss tangent

Figure 3: Effect of conductor and dielectric losses on propagation constant of the dominant microstrip mode as a function of frequency

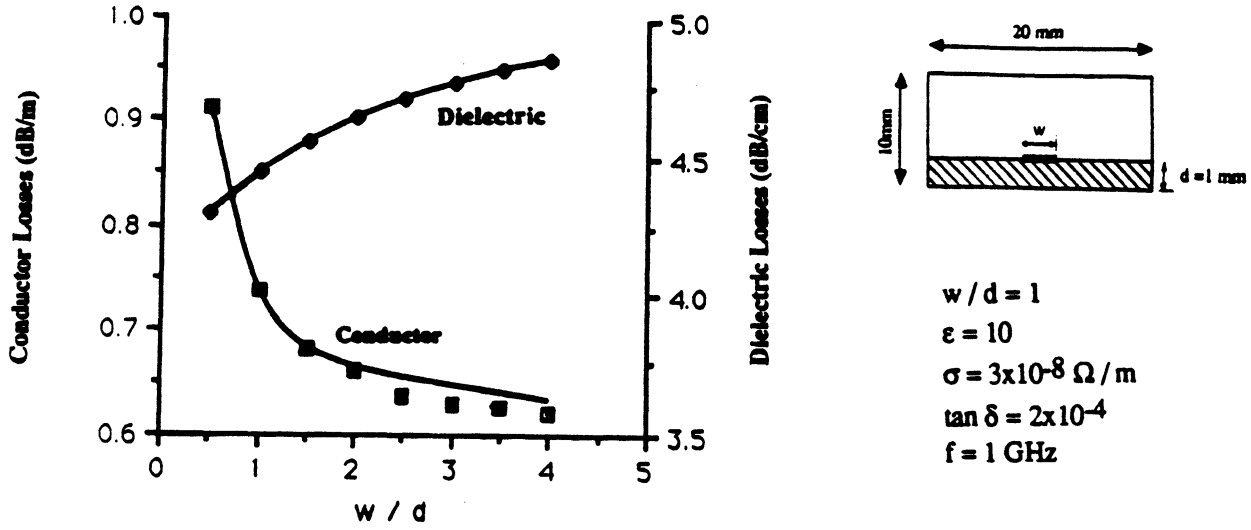

Figure 4: Conductor and dielectric losses of a single strip versus strip width: — present method, ⊡ results from [5]

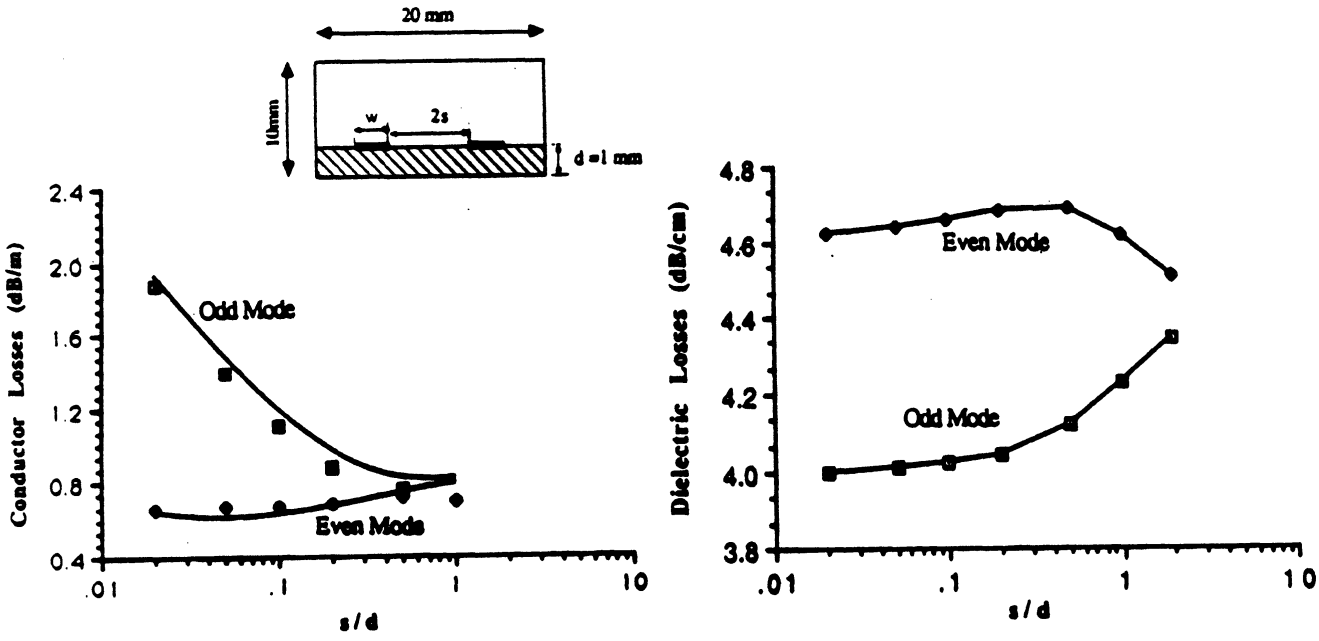

Figure 5: Conductor and dielectric losses of coupled strips versus line separation: — present method, □ results from [5]

ANALYSIS OF MULTILAYER IRREGULAR MICROSTRIP DISCONTINUITIES

William P. Harokopus, Jr., Pisti B. Katehi*

ABSTRACT

A full-electromagnetic analysis of open microstrip discontinuities on layered dielectric substrates is presented. The space domain method of moments formulation accounts fully for all electromagnetic coupling, and space and surface wave radiation. This versatile formulation has the potential to characterize an extensive variety of irregular, multi-dielectric layer microstrip structures.

INTRODUCTION

The steadily increasing demand for monolithic microwave and millimeter wave technology in space, military, and civilian applications is fueling the need for accurate microwave circuit computer-aided design. One particular area of importance is the electromagnetic modeling of passive microstrip circuit elements and discontinuities. When the microstrip circuits are not enclosed in waveguide housing or packaging, surface wave excitation and space wave radiation become important effects at millimeter wave frequencies. This is the case when microstrip elements are used in the feed networks of monolithic antenna arrays. In addition, multi-dielectric layers and dielectric overlays offer flexibility in the design of MMIC circuits and array feed networks. Consequently, the full electromagnetic characterization of multilayer microstrip is crucial.

In the past, full wave analysis has been applied primarily to electrically thin open microstrip discontinuities such as open ends or gaps on a single dielectric layer [1], [2], or with a dielectric overlay [3]. More recently, full-wave analysis has been performed on irregular microstrip discontinuities printed on a single layer including microstrip step, stub and corner discontinuities [4], [5]. Nonetheless, CAD packages for most microstrip discontinuities and elements such a T-junctions are based on quasi-static [6], dispersive [7], or semi-empirical techniques [8]. These methods fail to account for radiation and coupling. Irregular multi-dielectric layer structures have not been treated with full wave techniques. Therefore, much effort is needed in the development of microstrip CAD in the millimeter range.

The technique employed in this paper is a space domain method of moments solution of Pocklington's Integral equation. The procedure has proven effective for microstrip steps, stubs, and corners on a single dielectric layer [5]. Presented here is an extension to microstrip having substrates with multiple layers or with dielectric overlays. This

versatility is obtained by the application of the general space domain Green's function for an arbitrary multiple layer configuration. The proposed technique is directly applicable to a extraordinary variety of multilayer configurations including broadside couplers and filters, antenna elements fed by electromagnetically coupled transmission lines located on a different layer, and dielectric overlays. Numerical results for a two-layer microstrip corner will be presented and radiation losses will be discussed.

THEORY

A corner discontinuity on a multilayer substrate with an overlay is shown in Figure 1. The electric field from an irregular microstrip discontinuity on a general multi-dielectric layer substrate is given by Pocklington's integral equation

$$\bar{E}(r,\phi,z) = \int\int_{s'} \bar{\bar{G}}(r,r') \cdot \bar{J}(r')ds' \tag{1}$$

where $\bar{\bar{G}}$ is the dyadic green's function for a Hertzian dipole located above or within a grounded multi-dielectric substrate [9],[10]. A powerful advantage of this formulation lies in its ability to model an arbitrary number of substrate layers or a configuration having conducting strips on more than one interface, by using an iterative form for the space domain Green's function.

Both current components on the plane of the microstrip conducting strips are included. A two-dimensional application of Method of Moments [11] is used to discretize the integral equation over the element. The two current components are expanded into finite series of unknown current amplitudes and rooftop basis functions having piecewise sinusoidal variation in the longitudinal direction.

$$J_x = \sum_{n=1}^{N+1}\sum_{m=1}^{M+1} I^x_{nm} j^x_{nm}(x',y') \tag{2}$$

$$J_y = \sum_{n=1}^{N+1}\sum_{m=1}^{M+1} I^y_{nm} j^y_{nm}(x',y') \tag{3}$$

$$j^x_{n,m}(x',y') = [f_n(x')g_m(y')] \tag{4}$$

$$j^y_{n,m}(x',y') = [g_n(x')f_m(y')] \tag{5}$$

with

$$f_n(x') = \begin{cases} \frac{\sin k(x_{n+1}-x')}{\sin kl_x} & x_n \le x' \le x_{n+1} \\ \frac{\sin k(x'-x_{n-1})}{\sin kl_x} & x_{n-1} \le x' \le x_n \end{cases} \tag{6}$$

Table 1: Microstrip Corner Substrate Parameters

Case	ϵ_{r1}	ϵ_{r2}	$h_1(mil)$	$h_2(mil)$
A	10.2		40	0
B	2.2		40	0
C	2.2	10.2	20	20
D	10.2	2.2	20	20

and

$$g_m(y') = \begin{cases} 1 & y_{m-1} \leq y' \leq y_{m+1} \end{cases} \tag{7}$$

After substitution of the current expansions into the integral equation (1), the boundary condition for the tangential electric field on the conducting strip is enforced by Galerkin's method. A system of simultaneous equations results

$$\begin{bmatrix} Z_{xx} & Z_{xy} \\ Z_{yx} & Z_{yy} \end{bmatrix} \begin{bmatrix} I_x \\ I_y \end{bmatrix} = \begin{bmatrix} V_x \\ V_y \end{bmatrix} \tag{8}$$

where $Z_{ij}(i = x, y : j = x, y)$ represent blocks of the impedance matrix, I_i is the vector of unknown x and y current amplitudes, and V_j is the excitation vector which is identically zero everywhere except at the position of the source. After solution of the matrix equation, the current amplitudes on the feeding lines of the discontinuity are known. Figures 2 and 3 display the current on a corner discontinuity. Transmission line analysis is applied to determine the scattering parameters for the corner from the standing wave patterns on the feed lines.

NUMERICAL EXAMPLE

Shown in Figure 4, the scattering parameters for a microstrip corner discontinuity on a single layer are compared with the microwave CAD package *Touchstone*. At the higher frequency range, the effect of radiation losses can be seen in the discrepancy of S12 with the *Touchstone* results. This is due to the radiation losses which are not accounted for by *Touchstone*. A corner with the same physical dimensions was also characterized on substrates having two layers. Shown in Figure 5 are the scattering parameters of the two-layer problem as compared to a single layer of the higher permittivity material ($\epsilon_r = 10.2$). As illustrated, the reflection from the corner is strongly dependent on the properties of the substrate. The radiation properties of the corners are shown in Figure 6. In this frequency range it is believed that the losses come primarily from the TM_0 surface wave. The weaker radiation of the two-layer configuration with the higher permittivity material (Case D) on top, over the case of the lower permittivity

material (Case C) on top is believed to be related the suppression of surface wave modes reported by Jackson [12] for microstrip antennas. The tayloring of multilayer substrates for microstrip circuits in order to minimize surface wave losses will be explored further.

CONCLUSIONS

A full-wave Method of Moments formulation has been applied to a multilayer open microstrip corner. Utilizing an iterative form of the exact Green's function for a multilayer conductor backed medium, the procedure is applicable to a wide range of multilayer microstrip problems such as feed networks of monolithic antenna arrays. The method accounts fully for all electromagnetic coupling, dispersion, and radiation losses. Radiation losses of the corner discontinuity on several substrates are presented. The results demonstrate that multilayer substrates can be used to reduce surface wave losses.

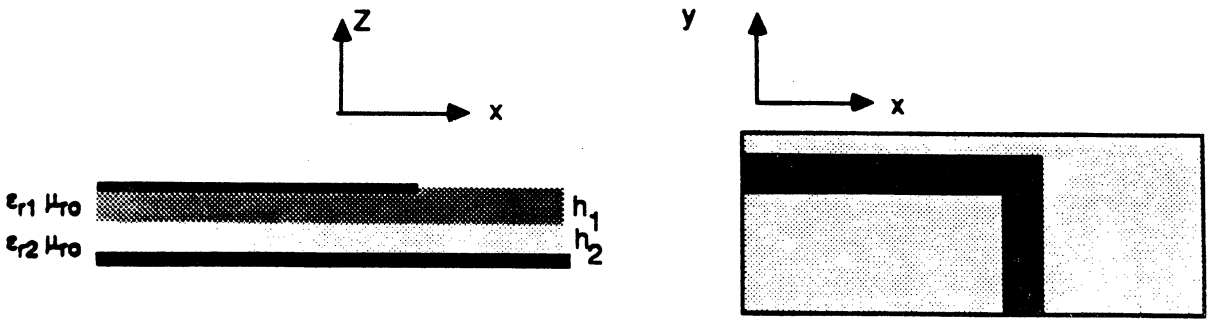

Figure 1: Open Microstrip Corner Discontinuity

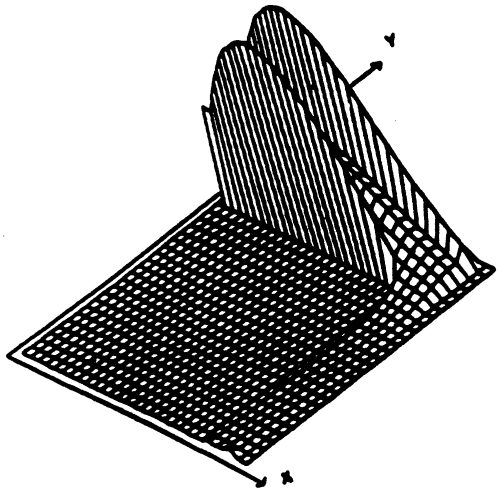

Figure 2: X-directed Current On Corner

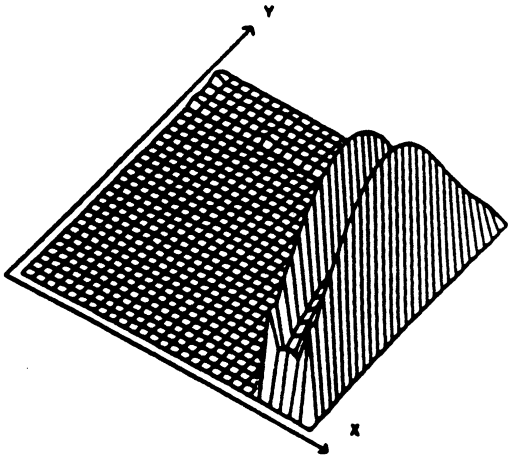

Figure 3: Y-directed Current On Corner

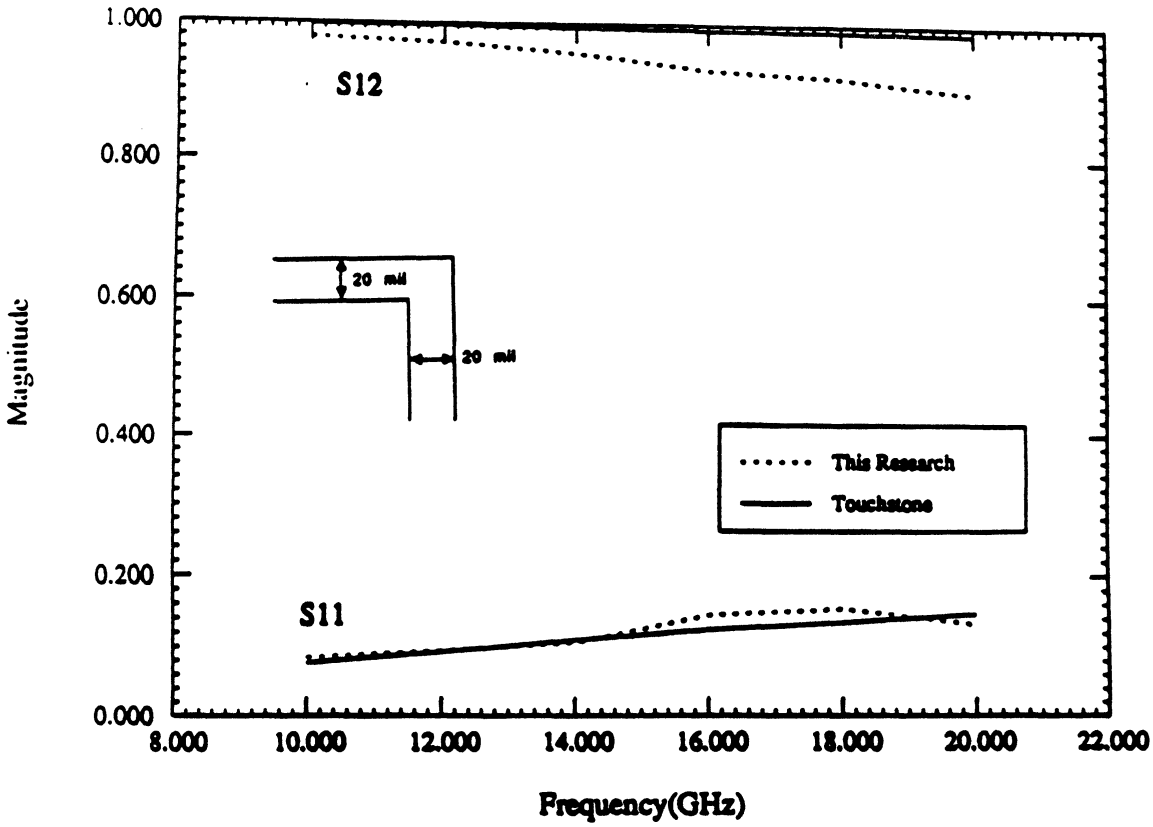

Figure 4: Scattering Parameters of Single Layer Corner

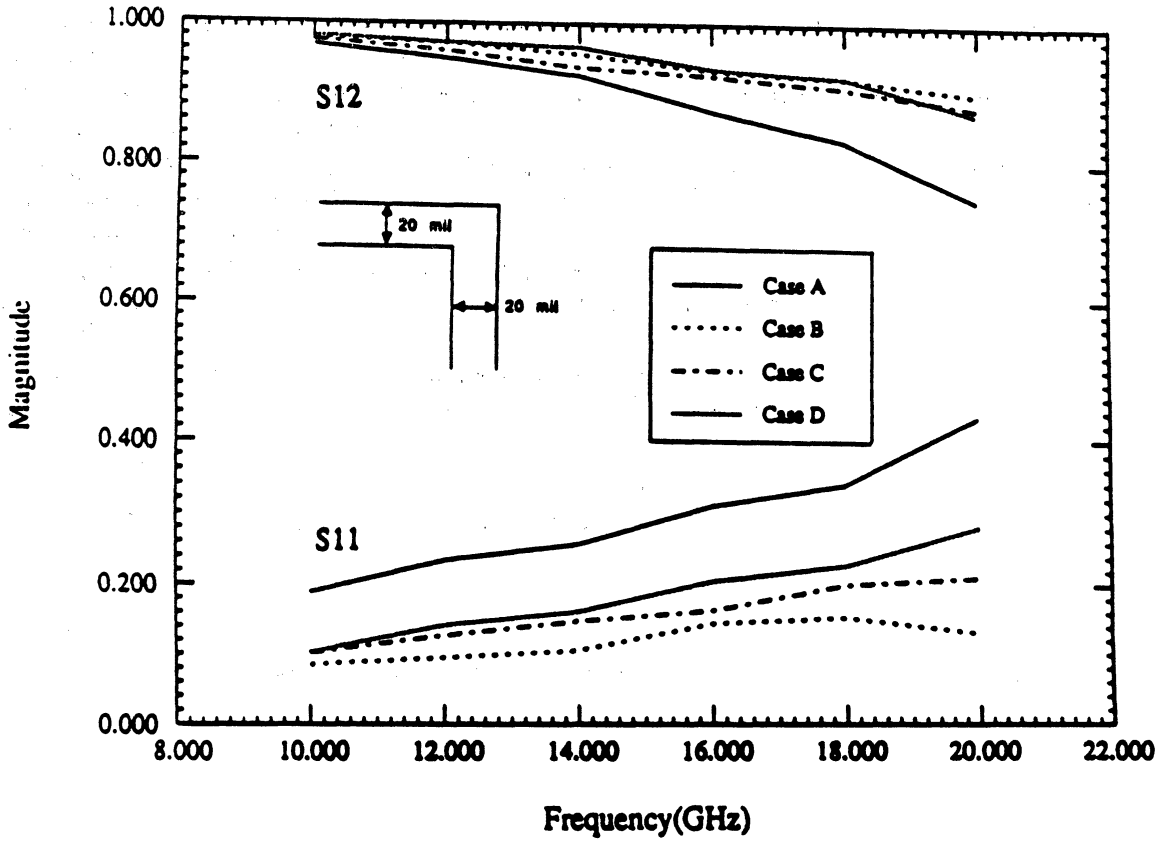

Figure 5: Scattering Parameters of Multilayer Corner

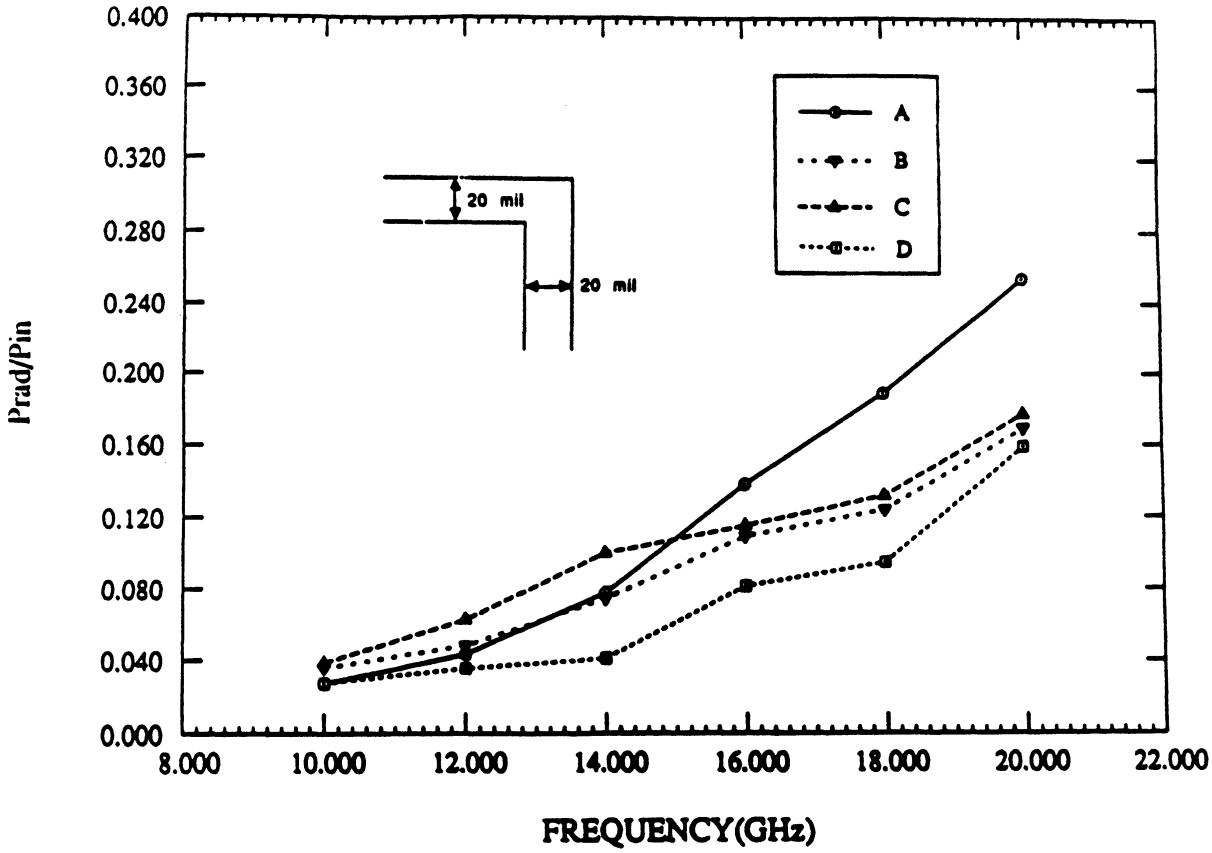

Figure 6: Radiation Properties of Microstrip Corner

References

[1] P.B. Katehi and N. G. Alexopoulos, "Frequency-Dependent Characteristics of Microstrip Discontinuities in Millimeter-Wave Integrated Circuits",*IEEE Trans. Microwave Theory Tech.*, Vol. MTT-33, No. 10, pp. 1029-1035.

[2] R. W. Jackson, and D. M. Pozar, "Full-Wave Analysis of Microstrip Open-End and Gap Discontinuities",*IEEE Trans. Microwave Theory Tech.*, Vol. MTT-33, No. 10, pp. 1036-1042.

[3] H. Yang, N. G. Alexopoulos, and D. R. Jackson, "Analysis of Microstrip Open-End and Gap Discontinuities in a Substrate-Superstrate Configuration," *IEEE MTT-S Microwave Symposium Digest*, 1988.

[4] R. Jackson, "Full-Wave Finite Element Analysis of Irregular Microstrip Discontinuities, *IEEE Trans. Microwave Theory Tech.*, Vol. MTT-37, No. 1, pp. 81-89.

[5] W. P. Harokopus, Jr. and P. B. Katehi, "An Accurate Characterization of Open Microstrip Discontinuities Including Radiation Losses", Accepted for publication to *1989 IEEE Microwave Symposium Digest.*

[6] P. Benedek and P. Silvester, "Equivalent Capacitance of Microstrip Gaps and Steps", *IEEE Trans. Microwave Theory Tech.*, Vol. MTT-20, 1972.

[7] I. Wolf, G. Kompa, and R. Mehran, "Calculation Method For Microstrip Discontinuities and T-Junctions," *Electron. Lett.*, Vol. 8, 1972.

[8] M. Kirschning, R.H. Jansen, and H.L. Koster, "Measurement and Computer-Aided Modeling of Microstrip Discontinuities by an Improved Resonator Method, 1983 "IEEE MTT-S International Microwave Symposium Digest", May, 1983.

[9] N.K. Das and D.M. Pozar, "A Generalized Spectral-Domain Green's Function for Multilayer Dielectric Substrates with Application to Multilayer Transmission Lines," *IEEE Trans. Microwave Theory Tech.*, Vol. MTT-35, No. 3, pp. 326-335.

[10] W. P. Harokopus, Jr. and P. B. Katehi, "An Accurate Characterization of Open Microstrip Discontinuities Including Radiation Losses", Submitted for publication to *IEEE Trans. Microwave Theory Tech.*.

[11] R. F. Harrington, Field Computation By Moment Methods,Macmillan,N.Y. ,1968.

[12] N.G. Alexopoulos, and D. R. Jackson, "Fundamental Superstrate (Cover) Effects on Printed Circuit Antennas," *IEEE Transactions on Antennas and Propogation*, Vol AP-32, No. 8, August 1984.

Acknowledgements

The research was sponsored by the Army Research Office (contract no. DAALO3-k- 0088 -23836-EL).

Characterization of Microstrip Discontinuities on Multilayer Dielectric Substrates Including Radiation Losses

Submitted to IEEE Transactions on Microwave Theory and Techniques
March, 1989
Revised-July 1989

William P. Harokopus, Jr. and Pisti B. Katehi
The Radiation Laboratory
Electrical Engineering and Computer Science Department
1301 Beal Ave.
University of Michigan, Ann Arbor MI., 48109
(313) 747-1796

Abstract-A two-dimensional space domain method of moments treatment of open microstrip discontinuities on multi-dielectric layer substrates is presented. The full-wave analysis accounts for electromagnetic coupling, radiation, and all substrate effects. The technique has been utilized to characterize commonly used discontinuities on one and two dielectric layers, and numerical results for step, corner, and

T-junction discontinuities are included.

1 Introduction

Monolithic circuit applications continue to extend farther into the millimeter-wave range approaching terahertz frequencies. At these frequencies, planar transmission line structures are required for passive component design. In particular, microstrip components are frequently utilized in MMIC circuit applications. Unfortunately, available microstrip CAD discontinuity and circuit element models fail to account for electromagnetic effects which become significant with increasing frequency. Without reliable CAD, microwave design engineers will face unacceptably lengthy development cycles.

The preponderance of the available microstrip CAD is based on quasi-static methods [1]-[6], equivalent waveguide models[7]-[10], and semi-empirical models [11]. These models require little computational effort, but fail to adequately account for electromagnetic coupling, radiation, and surface wave excitation. Quasi-static methods provide accurate characterization only at lower frequencies, while planar waveguide models contain limited information on dispersion.

Consequently, an analysis accounting for electromagnetic coupling, space wave, and surface wave radiation is required for the characterization of microstrip discontinuities, couplers, and matching elements at higher frequencies. Increasingly powerful computers and innovative techniques make full electromagnetic analysis a realistic alternative in the design of high frequency microstrip circuits. Full-wave analysis has already demonstrated accuracy in modeling simple microstrip discontinuities on single dielectric layers.

Often, microstrip discontinuities and elements are enclosed in a package or a

cavity. Jansen has performed the analysis of irregular covered microstrip elements with a spectral domain technique [12]. Shielded microstrip discontinuities such as open-ends, gaps, stubs [13], and coupled line filters [14] have been studied by the method of moments.

Nonetheless, microstrip is often used in the design of feeding networks for monolithic antenna arrays. Unlike shielded microstrip, open microstrip discontinuities are free to radiate. Also, the microstrip substrate supports surface wave modes. High frequency microstrip design requires a thorough understanding of these effects. Full electromagnetic solutions have been performed on open microstrip elements which are electrically thin such as open ends, gaps, and coupled lines [17],[18],[19]. These solutions are based on the thin strip approximation, and utilized one-dimensional method of moments. Under this assumption, the transverse current component gives a second order effect and may be neglected. In addition, an analysis of open-end and gap discontinuities in a substrate-superstrate configuration has been performed [20]. More recently, a spectral domain solution was applied to irregular step and stub elements on a single layer[21]. However, the characterization of these microstrip elements is far from complete. The fact that these elements are parts of antenna feeding networks necessitates a serious consideration of the coupling and radiation losses and their effect on the performance of the antenna. In addition, in monolithic arrays, multiple dielectric layers offer many advantages in design of feeding networks: they allow alternative solutions to circuit layouts or can provide protection in the form of superstrates. Furthermore, the appropriate combination of dielectric and semi-conducting materials can

create circuits with desirable properties such as slow-wave structures. This paper addresses, for the first time, the problem of accurate characterization of microstrip discontinuities on multilayer substrates and carefully studies these effect of this dielectric structures on circuit performance.

The presented full wave analysis is based on the application of two-dimensional method of moments in the space domain. The dyadic Green's function for a grounded multi-dielectric layer configuration is employed to develop an algorithm capable of analyzing structures with an arbitrary number of layers. Included in the solution are both transverse and longitudinal current components, allowing the treatment of a wide class of irregular microstrip elements including steps of width, corners, and T junctions. On the microstrip conductors, both current components are expanded by rooftop basis functions. Once the current distribution is evaluated, transmission line theory is employed to determine the network parameters.

Numerical results from this technique have demonstrated excellent agreement with measurement and the spectral domain technique in the case of single dielectric layers. Scattering parameters will be presented for corner, and T-junction discontinuities on one and on more complicated dielectric structures. In addition on a single layer, the more complex geometry of a meander line containing four coupled bends will be presented. The implemented method fully accounts for coupling, space and surface wave radiation, and all dispersive effects.

2 Analysis

Much of the published work on full wave analysis of open microstrip discontinuities has been limited to structures with strip widths much smaller than the microstrip wavelength ($w << \lambda_g$). Under this approximation, the transverse current component can be considered a second order effect and neglected [16]. Therefore, analysis was restricted to thin-strip discontinuities such as open ends, gaps, and coupled line filters. Obviously, the transverse current component is critical for the analysis of irregular structures such as steps in width, corners, and T-junctions, and is therefore included in this analysis.

The general multilayer open microstrip geometry is shown in Figure 1. The dielectric layers are considered lossless, but the development is not limited by this assumption. The conductors have infinite conductivity with the strip conductor being of finite thickness ($t << \lambda_g$). Maxwell's equations and the application of Green's identities yield Pocklington's integral equation for the electric field:

$$\vec{E}(\vec{r}) = \int\int_{S'} \bar{\bar{G}}(\vec{r},\vec{r}') \cdot \vec{J}(x',y')dx'dy' \tag{1}$$

where $\vec{E}(r)$ is the total electric field at the point $\bar{r} = (x,y,z)$, $\vec{J}(x',y')$ is the unknown current on the microstrip conducting strip, and $\bar{\bar{G}}(\vec{r},\vec{r}')$ is the dyadic Green's function for x and y-directed Hertzian dipoles above a grounded multilayer slab.

To provide for the most general solution possible, strip conductors may be located on any interface. A general, numerically efficient Green's function for an arbitrary number of layers may be derived by decomposing the fields into LSE

and LSM modes with respect to $\hat{z}$ [23]. Cylindrical symmetry may also be exploited by using a Hankel Transform in the transverse direction. This results in the one-dimensional boundary value problem, which may be simplified to a two-layer structure by using equivalent impedance boundaries as illustrated in Figure 2a. In Figure 2b, the equivalent transmission line model for this structure is shown, from which the impedance boundaries can be determined.

After application of the inverse Hankel Transform, the solution to the resulting boundary value problem is a compact, computationally efficient space domain Green's function. For a multilayer geometry with the strip conductor located on the top layer (at the dielectric-air interface) the components of the Green's function are given by:

$$\begin{aligned} G_{xx} = G_{yy} \quad &= \frac{\omega\mu_0}{2\pi}\int_0^\infty \lambda J_0(\lambda\rho)\frac{e^{-ju_0 z}}{f_1(\lambda,\epsilon_{r_1},h_1,\epsilon_{r_2},h_2,....)}d\lambda \\ &-\frac{1}{2\pi}\frac{d^2}{dx^2}\int_0^\infty \frac{J_0(\lambda\rho)}{\lambda}e^{-ju_0 z}\left[\frac{u_0 u_1}{\omega\epsilon_0}\frac{1}{f_2(\lambda,\epsilon_{r_1},h_1,\epsilon_{r_2},h_2,....)}\right. \\ &\left.-\frac{\omega\mu_0}{f_1(\lambda,\epsilon_{r_1},h_1,\epsilon_{r_2},h_2,....)}\right]d\lambda \end{aligned} \tag{2}$$

$$\begin{aligned} G_{xy} = G_{yx} \quad &= -\frac{1}{2\pi}\frac{d^2}{dxdy}\int_0^\infty \frac{J_0(\lambda\rho)}{\lambda}e^{-ju_0 z}\left[\frac{u_0 u_1}{\omega\epsilon_0}\frac{1}{f_2(\lambda,\epsilon_{r_1},h_1,\epsilon_{r_2},h_2,....)}\right. \\ &\left.-\frac{\omega\mu_0}{f_1(\lambda,\epsilon_{r_1},h_1,\epsilon_{r_2},h_2,....)}\right]d\lambda \end{aligned} \tag{3}$$

with $\rho = \sqrt{(x-x')^2+(y-y')^2}$. In equations (2),and (3) the semi-infinite integration is over the spectrum of spatial frequencies λ ($\lambda^2 = k_x^2 + k_y^2$), and the parameters $u_n, (n = 0, 1, ...)$ . . . are given in terms of λ by the following relation

$$u_n = \sqrt{k_n^2 - \lambda^2} \tag{4}$$

where k_n is the wavenumber in the n^{th} layer. In addition, in equations (2)-(3) the

functions $f_1(\lambda, \epsilon r_1, h1, ...))$ and $f_2(\lambda, \epsilon r_1, h1, ..))$ are the characteristic equations for the TE and TM surface wave modes respectively, and have the form

$$f_1(\lambda, \epsilon r_1, h1, ...)) = u_0 + u_1 \frac{(1 - \Gamma_{f2})}{1 + \Gamma_{f2}} \tag{5}$$

$$f_2(\lambda, \epsilon r_1, h1, ..)) = u_1 + \epsilon_{r1} u_0 \frac{(1 + \Gamma_{a2})}{(1 - \Gamma_{a2})} \tag{6}$$

where Γ_{a2} and Γ_{f2} are the reflection coefficients looking into the substrate as shown in Figure 2b. The surface wave characteristic equations contain all of the information for the dielectric layers not adjacent to the current source within the parameters $\Gamma_{a,f}$. For the case of a single layer the solution simplifies to the space domain Sommerfeld Green's function [24],[25].

$$G_{xx} = G_{yy} = \frac{\omega\mu_0}{2\pi} \int_0^\infty \lambda J_0(\lambda\rho) \frac{e^{-ju_0 z}}{f_1(\lambda, \epsilon_{r_1}, h_1)} - \frac{1}{2\pi} \int_0^\infty \frac{d^2}{dx^2} e^{-ju_0 z} \frac{J_0(\lambda\rho)}{\lambda}$$
$$\left[\frac{u_0 u_1}{\omega\epsilon_0} \frac{1}{f_2(\lambda, \epsilon_{r_1}, h_1)} - \frac{\omega\mu_0}{f_1(\lambda, \epsilon_{r_1}, h_1)}\right] \tag{7}$$

$$G_{xy} = G_{yx} = -\frac{1}{2\pi} \int_0^\infty \frac{d^2}{dxdy} e^{-ju_0 z} \frac{J_0(\lambda\rho)}{\lambda} \left[\frac{u_0 u_1}{\omega\epsilon_0} \frac{1}{f_2(\lambda, \epsilon_{r_1}, h_1)} - \frac{\omega\mu_0}{f_1(\lambda, \epsilon_{r_1}, h_1)}\right] \tag{8}$$

where

$$f_1(\lambda, \epsilon_{r1}, h_1) = u_0 + u_1 \coth u_1 h_1 \tag{9}$$

$$f_2(\lambda, \epsilon_{r1}, h_1) = \epsilon_r u_0 + u_1 \tanh u_1 h_1 \tag{10}$$

where in the above, ϵ_{r1} is the relative dielectric constant, and h_1 is the thickness of the substrate.

The method of moments [26] is applied to transform Pocklington's integral equation to a system of linear equations. The microstrip discontinuity is subdivided into overlapping squares. The transverse and longitudinal current components on

the microstrip are expanded over these squares by finite series

$$J_x = \sum_{n=1}^{N+1} \sum_{m=1}^{M+1} I_{nm}^x j_{nm}^x(x', y') \tag{11}$$

$$J_y = \sum_{n=1}^{N+1} \sum_{m=1}^{M+1} I_{nm}^y j_{nm}^y(x', y') \tag{12}$$

where

$$j_{n,m}^x(x', y') = [f_n(x') g_m(y')] \tag{13}$$

$$j_{n,m}^y(x', y') = [g_n(x') f_m(y')] \tag{14}$$

In equations (11) and (12), I_{nm} is the unknown current amplitude at the $(n, m)^{th}$ position of the subdivided element. The functions f_n and g_m are sub-domain shaping or basis functions and are consistent with the current boundary conditions. The sub-domain basis functions have piecewise sinusoidal variation in the longitudinal direction and constant variation in the transverse direction according to

$$f_n(x') = \begin{cases} \frac{\sin k(x_{n+1} - x')}{\sin k l_x} & x_n \leq x' \leq x_{n+1} \\ \frac{\sin k(x' - x_{n-1})}{\sin k l_x} & x_{n-1} \leq x' \leq x_n \\ 0 & Else \end{cases} \tag{15}$$

and

$$g_m(y') = \begin{cases} 1 & y_{m-1} \leq y' \leq y_{m+1} \\ 0 & Else \end{cases} \tag{16}$$

In the above, $l_x = x_{n+1} - x_n$, and k is a scaling parameter chosen to vary between k_0 (free space wavenumber) and k (wavenumber in the dielectric). The numerical solution has shown that best stability occurs when the scaling constant is chosen close to the guide wavelength. Substitution of the above into Pocklington's integral

equation (1) yields a system of linear equations in the form

$$E_x + \Delta E_x = \sum_{n=1}^{N+1} \sum_{m=1}^{M+1} Z_{xx}^{nm} I_x^{nm} + Z_{xy}^{nm} I_y^{nm} \tag{17}$$

$$E_y + \Delta E_y = \sum_{n=1}^{N+1} \sum_{m=1}^{M+1} Z_{yx}^{nm} I_x^{nm} + Z_{yy}^{nm} I_y^{nm} \tag{18}$$

where $Z_{ij}^{nm}(i,j = x,y)$ constitutes the contribution of the j^{th} component of current to the i^{th} component of the electric field from the current element on the $(nm)^{th}$ sub-division. The terms ΔE_x and ΔE_y represent the errors in the electric field due to the approximations made in the current.

During the derivation of the Green's function, all applicable boundary conditions for the grounded multi-dielectric geometry were applied with the exception of the condition on the microstrip conductors. This condition, which states that the tangential electric field has to go to zero on the surface of the conducting strips, will be enforced through the method of moments procedure. In addition, it has been shown that Galerkin's procedure represents a strong condition on the minimization of the errors ΔE_x and ΔE_y. For this procedure, the following inner products are defined

$$V_{\nu\mu}^x = \langle j_{\nu\mu}(\vec{r}), E_x \rangle = \int_{x_{n-1}}^{x_{n+1}} \int_{y_{m-1}}^{y_{m+1}} (E_x + \Delta E_x) f_\nu(x) g_\mu(y) dx dy \tag{19}$$

$$V_{\nu\mu}^y = \langle j_{\nu\mu}(\vec{r}), E_y \rangle = \int_{x_{n-1}}^{x_{n+1}} \int_{y_{m-1}}^{y_{m+1}} (E_y + \Delta E_y) f_\nu(y) g_\mu(x) dx dy \tag{20}$$

where $f_\nu(x)$ and $g_\mu(y)$ are testing functions identical to the basis functions and $(\nu = 1, ..., N+1, \mu = 1, ..., M+1)$. In view of (19),(20) equations (17),(18) result in the following matrix equation.

$$\begin{bmatrix} ZXX_{nm}^{\nu\mu} & ZXY_{nm}^{\nu\mu} \\ ZXX_{nm}^{\nu\mu} & ZYY_{nm}^{\nu\mu} \end{bmatrix} \begin{bmatrix} I_x^{nm} \\ I_y^{nm} \end{bmatrix} = \begin{bmatrix} V_{\nu\mu}^x \\ V_{\nu\mu}^y \end{bmatrix}$$

where $ZIJ^{\nu\mu}_{nm}(I,J = X,Y)$ represent blocks of the impedance matrix, I_i is the vector of unknown x and y current amplitudes, and V_j is the excitation vector which is identically zero everywhere except at the position of the source. Once the matrix inversion is performed, the current amplitudes on the feeding lines are known.

In order to extract the scattering parameters, the discontinuity, is excited systematically at all ports by delta gap generators. Assuming a unimodal field excited on the microstrip feeding line, beyond a reference plane the current forms TEM-like standing waves. Transmission line theory can then be used to extract the scattering parameters for a network from the standing wave patterns on the feeding lines. The presence of the gap is reflected in the excitation vector where

$$V_x^{\nu\mu} = \begin{cases} 1 & if \quad x_\nu = x_g \\ 0 & Else \end{cases} \tag{21}$$

and

$$V_y^{\nu\mu} = \begin{cases} 1 & if \quad y_\mu = y_g \\ 0 & Else \end{cases} \tag{22}$$

In the above, x_g and y_g are positions of an x-oriented and y-oriented gap generators respectively.

In Figure 3, the three-dimensional plot depicts the current on a T-junction excited at all three of its ports by gap generators. As illustrated, the current assumes a uniform standing wave pattern along the feeding lines of the discontinuity. With a longer length of feed line then shown, the current SWR and positions of minima

can be determined. The considered minima are away from the discontinuity, far enough for higher order modes to have vanished. The reflection coefficient at a reference plane $X = L$, looking in any port is

$$\Gamma(L) = \frac{SWR - 1}{SWR + 1} e^{j\frac{-4\pi(L - X_{min})}{\lambda_g}} \tag{23}$$

where SWR is the current standing wave ratio, and X_{min} is the position of a current minimum. The microstrip guide wavelength λ_g has been previously determined from a long open ended line.

From the reflection coefficient, the normalized input impedance may be determined according to

$$Z_{in} = \frac{1 + \Gamma(L)}{1 - \Gamma(L)} \tag{24}$$

To evaluate the network parameters an N-port discontinuity must be excited by N independent excitations. In the case of a symmetrical 2-port, even and odd excitations may be employed. For the even case the gap generators are of equal magnitude and phase, and for the odd case they have equal magnitude and are out of phase by 180 degrees. The even and odd input impedances, obtained from equations (23),and (24), may be combined to give the elements for the Z-matrix which for the case of a symmetric network take the form

$$Z_{11} = \frac{Z_{in}^{1e} + Z_{in}^{1o}}{2} \tag{25}$$

$$Z_{22} = Z_{11} \tag{26}$$

$$Z_{12} = \frac{Z_{in}^{1o} - Z_{in}^{1e}}{2} \tag{27}$$

$$Z_{12} = Z_{21} \tag{28}$$

In the above, $Z_{in}^{1e(o)}$ refers to port 1 under an even(odd) excitation. For non-symmetric networks, and multiport networks similar expressions may be obtained. The scattering parameters are obtained from the Z-matrix by a simple transformation.

Finally, the total radiation losses may be determined from the known relation:

$$\frac{P_{rad}}{P_{in}} = 1 - |S_{11}|^2 - |S_{12}|^2 \tag{29}$$

3 Evaluation of Impedance Matrix Elements

The numerical evaluation of the Sommerfeld integrations involved in the Green's function is quite involved. A detailed discussion of the evaluation of the Sommerfeld integrations has been included in the author's previous work [29] and will not be discussed further here.

In the matrix equation of section 2 the terms $ZXX_{nm}^{\nu\mu}$ and $ZYY_{nm}^{\nu\mu}$ represent the interactions between the x or y components located in the $(n,m)^{th}$) and $(\nu,\mu)^{th}$) cells. The terms $ZXY_{nm}^{\nu\mu}$ and $ZYX_{nm}^{\nu\mu}$ represent the interaction between the x and y components located in the $(n.m)^{th}$) and $(\nu.\mu)^{th}$) cells. The computation of all of the $2(NM)^2$ interactions would be extremely time-consuming. Yet, the number of computations can be greatly reduced noting the following points. For the direct-coupled blocks, due to the symmetry and the even valueness of the Green's function with respect to the x and y separations, all interactions between subsections depend only on the magnitudes $|x - x'|$ and $|y - y'|$. For the cross-coupled blocks, the symmetry and the odd valueness of the Green's functions may lead to similar conclusions. Thus, vectors of impedance matrix elements may be

precomputed and catalogued according to separations for various substrates and subsection sizes. These "libraries" can then be used repeatedly for discontinuity analysis.

A typical impedance matrix is plotted in Figure 4. As illustrated, the matrix is toplitz with the diagonal elements being the largest by an order of magnitude. Although not done in the following results, it appears evident from the figure that interactions of subsections electrically distant may be ignored. This could result in further savings in computer time.

4 Numerical Results

4.1 Single Layer Discontinuities

The presented technique has been applied to characterize the discontinuity shown in figure 5a. This matching section is printed on a 10 mil substrate of relative permittivity 9.9. Over the frequency range of interest, the microstrip section and substrate thickness are electrically small ($< \frac{1}{10} \lambda_g$). As expected, our moment method algorithm has found radiation losses insignificant for this example. Figures 5a and 5b show the magnitude and phase of the scattering parameters as compared to measurement. As illustrated, the agreement with measurements for magnitude and phase is excellent. In particular, the agreement of the phase is within 2.5 degrees across this frequency range. The measurements were performed by TI using a cascade prober and an 8510 automatic network analyzer.

4.1.1 Radiation Losses

Radiation losses for open microstrip elements can be significant at millimeter-wave frequencies. To illustrate the ability of the presented analysis to account for space and surface wave losses, a microstrip stub on a single microstrip layer was compared to previously published data obtained with the spectral domain technique[21]. The microstrip stub, contains a T-junction discontinuity and an open end, and is printed on a 1.27 mm substrate of dielectric constant 10.65. As illustrated in figure 6, the agreement between our space domain technique and the spectral domain technique is very good. The quantity denoted G in the graph corresponds to $|S_{11}|^2 + |S_{12}|^2$, which may be subtracted from 1 to determine the total radiated power. The quarter wave resonance occurs just beyond 10 GHz. Also included in the plot are measurements obtained by Jackson[21].

4.1.2 Single Loop Meander Line

Multi-loop meander lines are frequently used in MMICS, such as traveling wave amplifiers, for their slow-wave properties. The formulation presented in this paper has been applied to simulate a single loop meander line in order to illustrate the versatility of the method in modeling irregular microstrip discontinuities. Furthermore, the consideration of a single loop instead of a multi-loop line speeds up the computation and reveals very explicitly the effect of distributed discontinuities and electromagnetic coupling on the slow-wave properties of the structure.

The line is printed on a 10 mil alumina substrate ($\epsilon_r = 9.9$). The magnitude of S_{21} is shown in Figure 7 as a function of frequency for three values of the width

to spacing ratio ($\frac{w}{s}$). In addition, Figure 8 shows the normalized phase velocity around the loop (v'/v) as a function of frequency where v is the phase velocity on a microstrip line of length equal to the mean path length of the loop. These results indicate, in this frequency range, that the parasitics in the loop increase the phase velocity v' which in turn tends to reduce the overall slow-wave effect of the meander line.

4.2 Multilayer Microstrip Discontinuities

A powerful advantage of the presented formulation is the ability to model multlayer substrates by replacing the single layer Green's function with the multi-layer function. The fullwave procedure was applied to a microstrip corner discontinuity on a substrate having two dielectric layers. The magnitude of the scattering parameters is shown in Figure 9. The multilayer corner has been analyzed on four different substrates: A) a 40 mil layer of alumina ($\epsilon_r = 10.2$), B) a 40 mil layer of duroid ($\epsilon_r = 2.2$), C) a 20 mil layer duroid on a 20 mil layer of alumina, and D) A 20 mil layer of alumina on a 20 mil layer of duroid.

There is significant difference in radiation between the two multilayer cases. The radiation from the structure having duroid over alumina is considerably more than the structure having alumina over duroid, as illustrated in Figure 10. It is believed that for this structure, the loss is primarily due to surface wave radiation. Therefore, case D couples less power into surface waves than case C. This phenomenon is believed to be related to the suppression of surface wave excitation reported by D. Jackson [27] in his study of antenna elements.

A two-layer microstrip stub was also analyzed. Shown in Figure 11 is the

magnitude of the scattering parameters for a stub on substrate having a layer of GaAs ($\epsilon_r = 12.2$) on Quartz ($\epsilon_r = 4.0$). Both layers are .2 mm thick. Also included are the scattering parameters for a stub having the same dimensions on a single layer of quartz. The single layer example has a resonant frequency at 41 GHz. The higher effective dielectric constant for the 2-layer case creates a stub having a smaller resonant length, and results in a downward shift in frequency for the null of $|S12|$. The radiation losses for both stubs are included in Figure 12. As illustrated, the multilayer stub shows a tendency to radiate less. This indicates that multilayer substrates may be utilized to reduce radiation losses.

5 Conclusion

A versatile analysis of microstrip discontinuities has been presented. The two-dimensional method of moments technique has demonstrated excellent agreement with measurements and other theoretical data derived for a single layer. A powerful extension of the method allows the treatment of discontinuities on more complicated dielectric structures. This is accomplished by employing the Green's function for a conductor backed multi-dielectric layer, resulting in the ability to model with full electromagnetic analysis an abundant variety of nonuniform microstrip configurations.

Numerical results for corner, and T-junction discontinuities have been presented on two dielectric layers. Additionally, the formulations ability to model larger elements composed of these building blocks has been demonstrated by the inclusion of a design curve for a meander line.

The fullwave technique accurately accounts for coupling, space wave, and surface wave radiation. Curves of radiation losses are presented for the corner and stub elements.

Acknowledgement

This research was sponsored by the National Science Foundation Grant ECS-8602536 and the Army Research Office (contract no. DAALO3-k-0088[23836-EL]). The authors gratefully acknowledge Dr. S.R. Nelson and Mr. A. Crane of Texas Instruments for their contributions to this work.

References

[1] M. Maeda, "Analysis of Gap in Microstrip Transmission Lines", *IEEE Trans. Microwave Theory Tech.*, Vol. MTT-20, pp.390-396, Jun. 1972.

[2] P. Benedek and P. Silvester, "Equivalent Capacitance of Microstrip Gaps and Steps", *IEEE Trans. Microwave Theory Tech.*, Vol. MTT-20, pp.729-733, Nov. 1972.

[3] P. Silvester and P. Benedek, "Equivalent Capacitance of Microstrip Open Circuits," *IEEE Trans. Microwave Theory Tech.*, Vol. MTT-20, pp. 511-516, Aug. 1972.

[4] P. Silvester and P. Benedek, "Equivalent discontinuities capacitances for Right-Angle Bends, T-junctions, and Crossings," *IEEE Trans. Microwave Theory Tech.*, Vol. MTT-21, pp. 341-346, May 1973.

[5] R. Horton, "The Electrical Characterization of a Right-Angle Bends in Microstrip Line," *IEEE Trans. Microwave Theory Tech.*, Vol. MTT-21, pp.427-429, Jun. 1973.

[6] C. Gupta, A. Gopinath "Equivalent circuit capacitance for microstrip change in width", it IEEE Trans. Microwave Theory Tech., Vol. MTT-25, pp.819-821, Oct. 1977.

[7] T. Itoh, "Analysis of Microstrip resonators", *IEEE Trans. Microwave Theory Tech.*, Vol. MTT-22, pp.946-952, Nov. 1974.

[8] I. Wolf, G. Kompa, and R. Mehran, "Calculation Method For Microstrip Discontinuities and T-Junctions," *Electron. Lett.*, Vol. 8, 1972.

[9] G. Kompa, and R. Mehran, "Planar Waveguide Model For Calculating Microstrip Components," *Electron. Lett.*, Vol. 11, 1975.

[10] W. Menzel and I. Wolf, "A Method For Calculating the frequency Dependent Properties of Microstrip Discontinuities," *IEEE Trans. Microwave Theory Tech.*, Vol. MTT-25, pp. 107-112, Feb. 1977.

[11] M. Kirschning, R.H. Jansen, and H.L. Koster, "Measurement and Computer-Aided Modeling of Microstrip Discontinuities by an Improved Resonator Method, 1983 "IEEE MTT-S International Microwave Symposium Digest", May, 1983.

[12] R. H. Jansen, "The Spectral Domain Approach for Microwave Integrated Circuits," *IEEE Trans. Microwave Theory Tech.*, Vol. MTT-33, pp.1043-1056, Oct. 1985.

[13] J. C. Rautio and R.F. Harrington, "An electromagnetic timeharmonic analysis of shielded microstrip circuits," *IEEE Trans. Microwave Theory Tech.*, Vol. MTT-35, pp. 726-730, Aug. 1987.

[14] L. P. Dunleavy and P. B. Katehi, "A Generalized Method for Analyzing Shielded Thin Microstrip Discontinuities ," *IEEE Trans. Microwave Theory Tech.*, Vol. MTT-36, pp.178-1766, Dec. 1988.

[15] L. P. Dunleavy and P.B. Katehi,"Shielding Effects in Microstrip Discontinuities," *IEEE Trans. Microwave Theory Tech.*, Vol. MTT-36, pp.1767-1774, Dec. 1988.

[16] P.B. Katehi and N. G. Alexopoulos, "On the Effect of Substrate Thickness and Permittivity and Permittivity On Printed Circuit Dipole performance," *IEEE Transactions on Antennas and Propagation*, Vol AP-31, pp. 34-38, Jan. 1983.

[17] N. G. Alexopoulos, P.B. Katehi, and D. Rutledge, "Substrate Optimization for Integrated Circuit Applications," *IEEE Trans. Microwave Theory Tech.*, Vol. MTT-31, pp. 550-557, July, 1983.

[18] P.B. Katehi and N. G. Alexopoulos, "Frequency-Dependent Characteristics of Microstrip Discontinuities in Millimeter-Wave Integrated Circuits",*IEEE Trans. Microwave Theory Tech.*, Vol. MTT-33, Oct. 85, pp. 1029-1035.

[19] R. W. Jackson, and D. M. Pozar, "Full-Wave Analysis of Microstrip Open-End and Gap Discontinuities",*IEEE Trans. Microwave Theory Tech.*, Vol. MTT-33,Oct. 85, pp. 1036-1042.

[20] H. Yang, N. G. Alexopoulos, and D. R. Jackson, "Analysis of Microstrip Open-End and Gap Discontinuities in a Substrate-Superstrate Configuration," *IEEE MTT-S Microwave Symposium Digest*, pp. 705-708, June 1988.

[21] R. Jackson, "Full-Wave Finite Element Analysis of Irregular Microstrip Discontinuities, *IEEE Trans. Microwave Theory Tech.*, Vol. MTT-37, pp. 81-89, Jan. 89.

[22] W. P. Harokopus, Jr. and P. B. Katehi, "An Accurate Characterization of Open Microstrip Discontinuities Including Radiation Losses", *IEEE Microwave Symposium Digest*, pp. 231-234, June 1989.

[23] N.K. Das and D.M. Pozar, "A Generalized Spectral-Domain Green's Function for Multilayer Dielectric Substrates with Application to Multilayer Transmission Lines," *IEEE Trans. Microwave Theory Tech.*, Vol. MTT-35, pp.326-335, March 1987.

[24] A. Sommerfeld, Partial Differential Equations in Physics, New York, N.Y., Academic Press, 1949.

[25] R.S. Elliott, "The Green's Function For Electric Dipoles Parallel To and Above or Within a Grounded Dielectric Slab", Hughes Technical Correspondence, 1978.

[26] R. F. Harrington, Field Computation By Moment Methods, Macmillan,N.Y. ,1968.

[27] N.G. Alexopoulos, and D. R. Jackson, "Fundamental Superstrate (Cover) Effects on Printed Circuit Antennas," *IEEE Transactions on Antennas and Propagation*, Vol AP-32, No. 8, pp. 807-814, August 1984.

[28] W. Wertgen, and R.H. Jansen, "Spectral Iterative Techniques For The Full-Wave 3-D Analysis of (M)MIC Structure," IEEE MTT-S Symposium Digest , pp.709-712, June 1988.

[29] P.B. Katehi and N. G. Alexopoulos, "Real Axis Integration of sommerfeld Integrals With Applications To Printed Circuit Antennas," *J. Math. Phys.*, vol. 24(3), Mar. 1983.

List of Figures

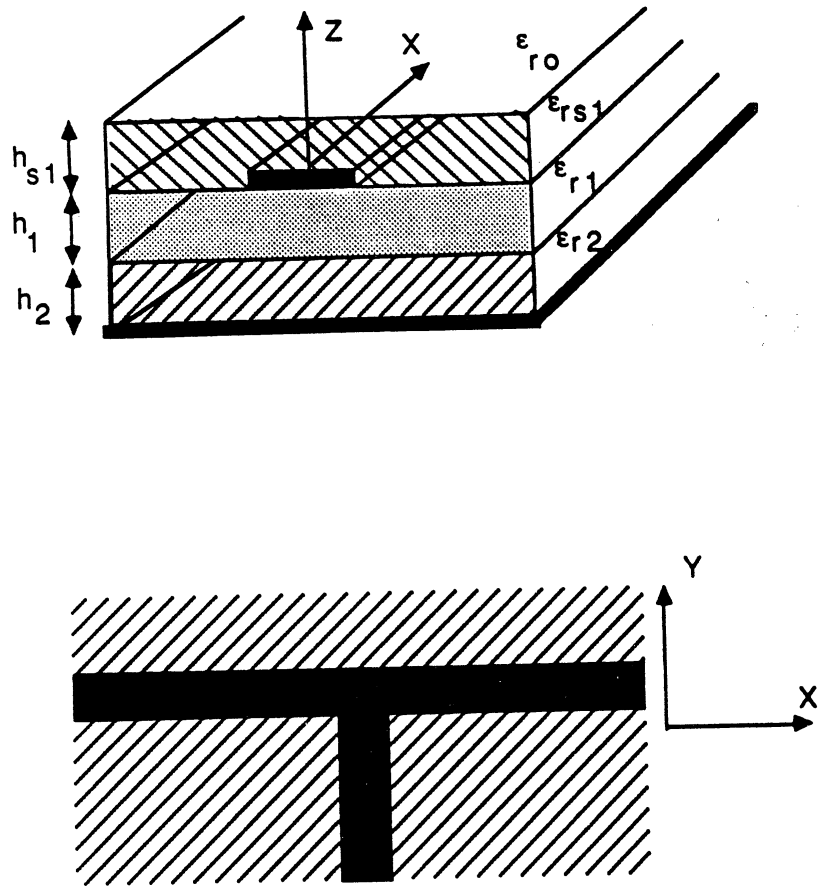

Figure 1: Multilayer Open Microstrip Geometry

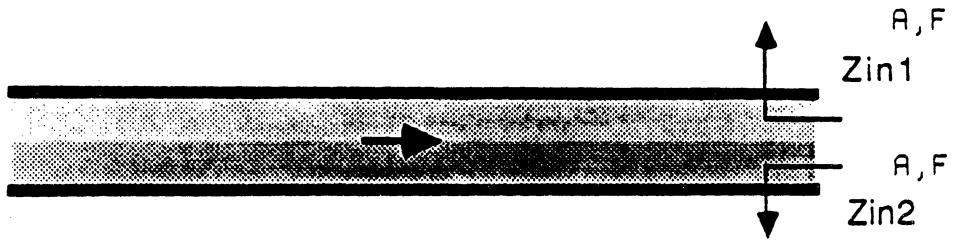

a. Equivalent Impedance Boundaries

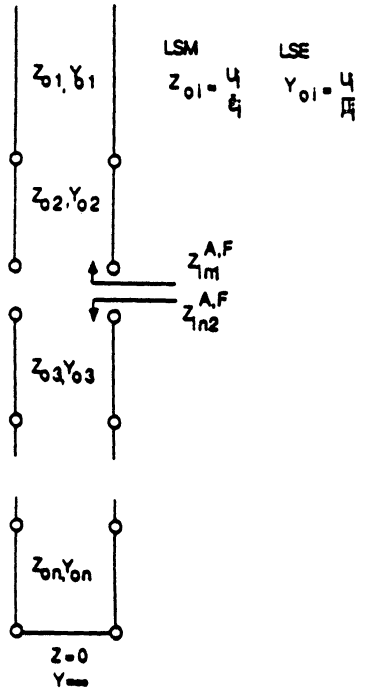

b. Transmission Line analogue

Figure 2: Derivation of General Multilayer Green's Function

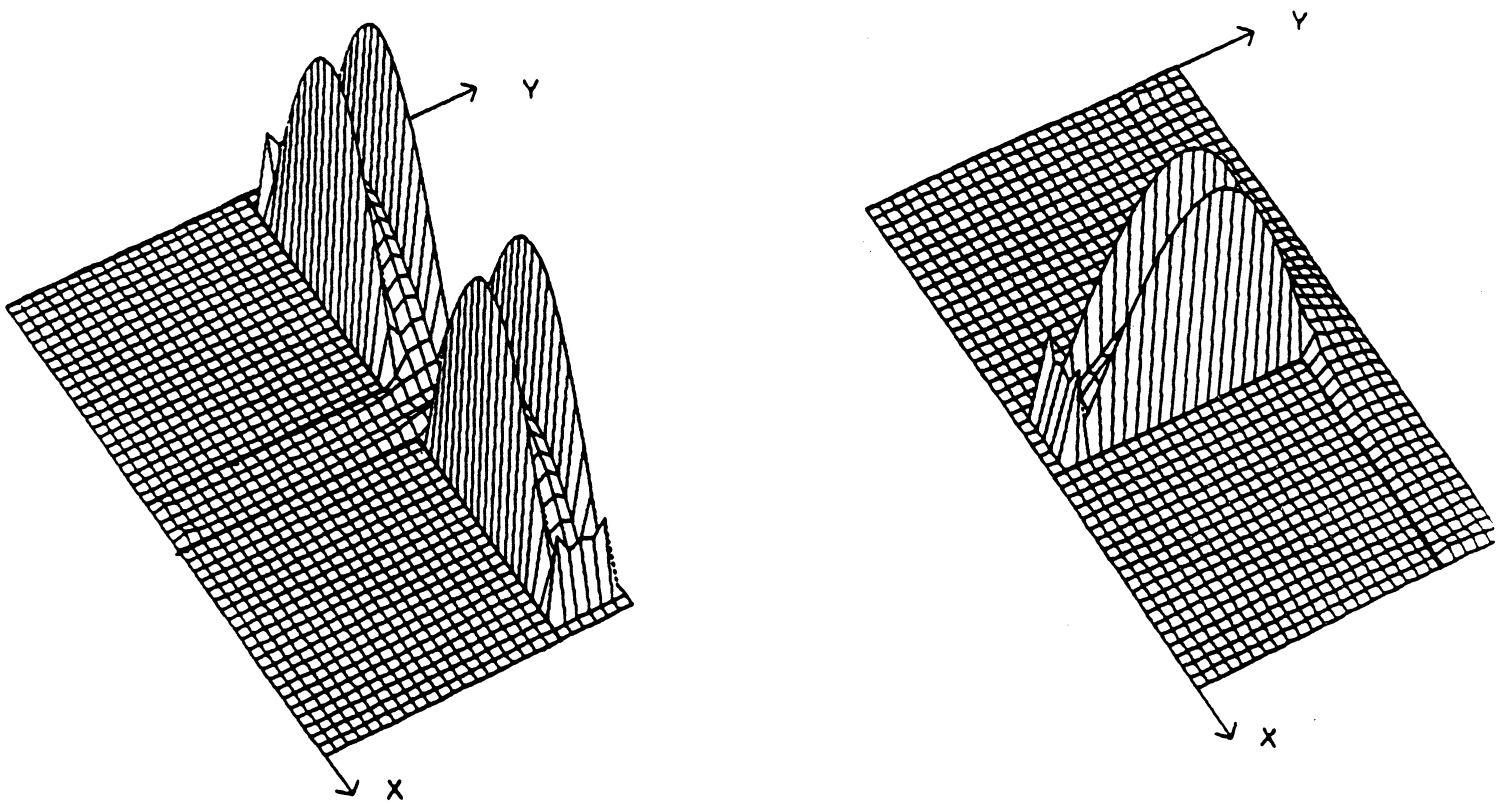

Figure 3: Current On T-Junction Excited by Gap Generators (ϵ_r=4, h=.4 mm, W=.2 mm)

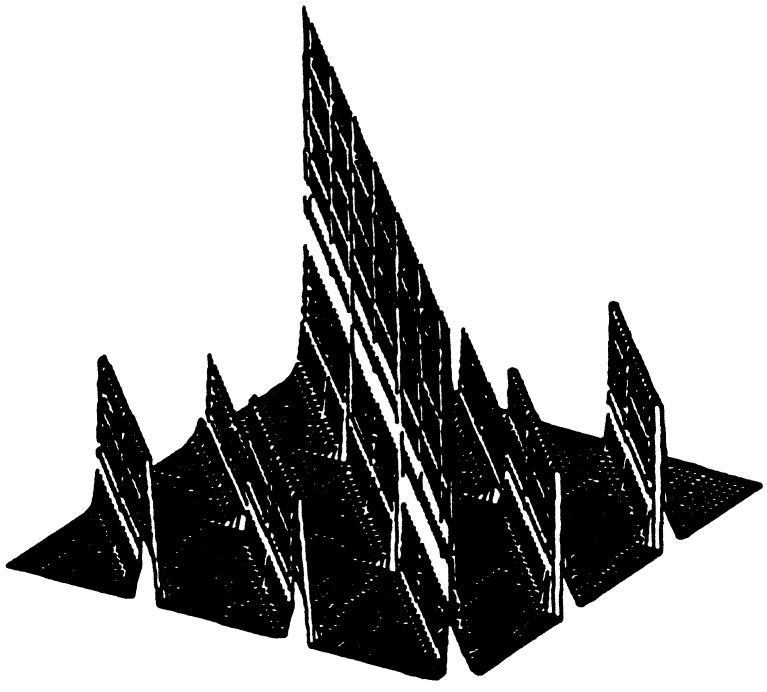

Figure 4: Toplitz Impedance Matrix

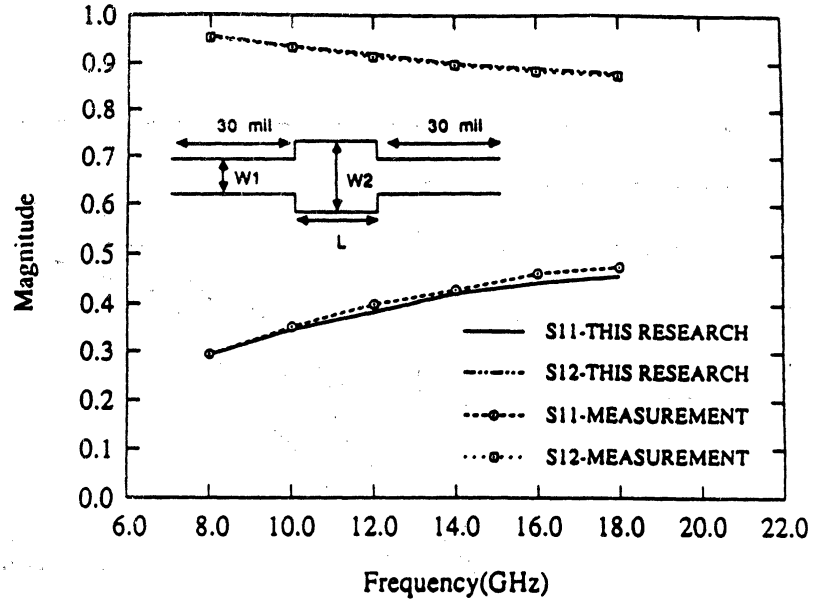

a. Ma

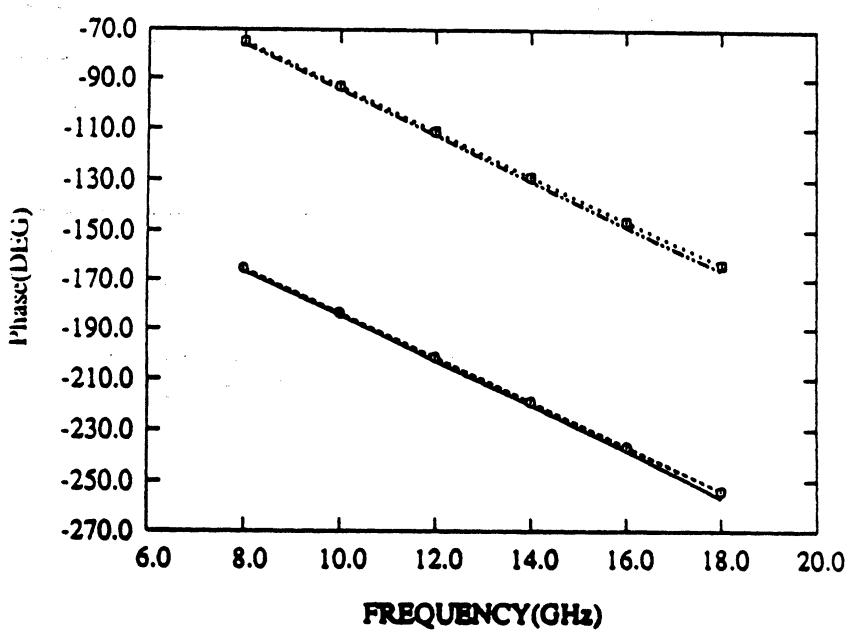

b. Phase

Figure 5: Scattering Parameters of Matching Section, numerical(experimental) dimensions: W1=9.2(9.2) mm, W2=23(23.1)mm, L=50.6(50.0), ϵ_r=9.9, h=10 mil

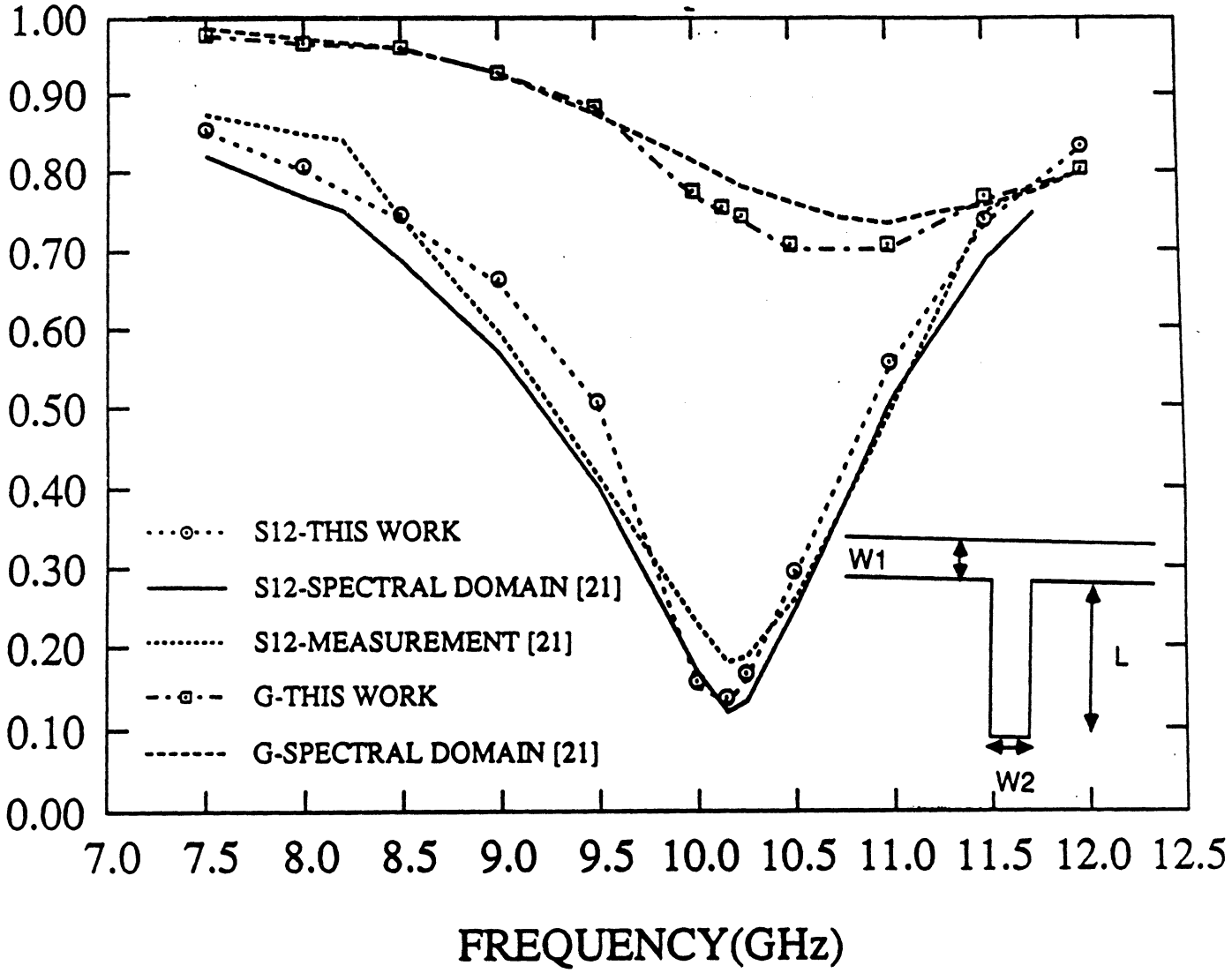

Figure 6: Scattering Parameters for Microstrip Stub, space(spectral) dimensions: W1=1.44(1.40), W2=1.44(1.40), L=2.16(2.16), ϵ_r=10.65, h=1.27 mm

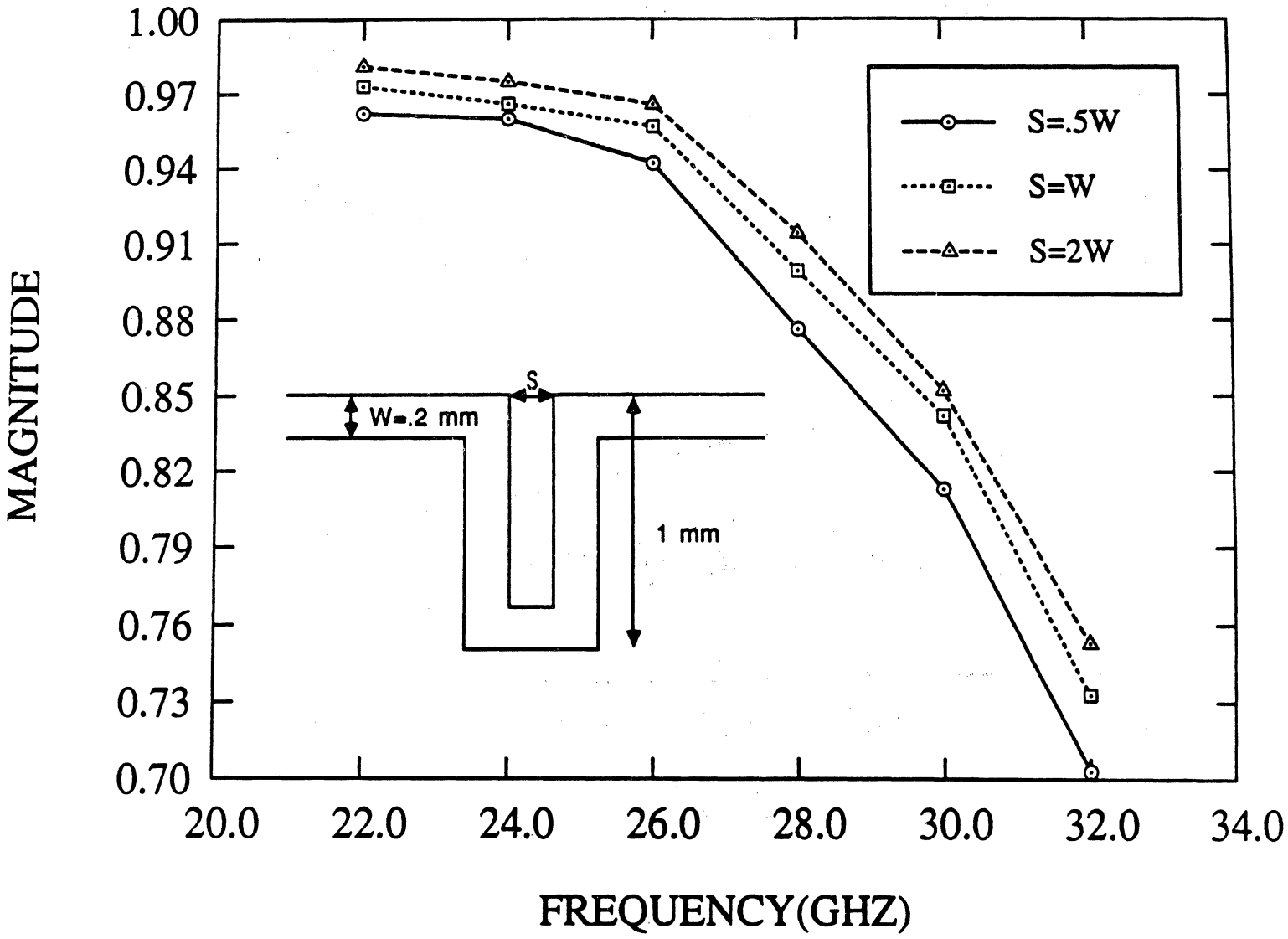

Figure 7: Design Curve for Meander Line ϵ_r=9.9, h=10 mil

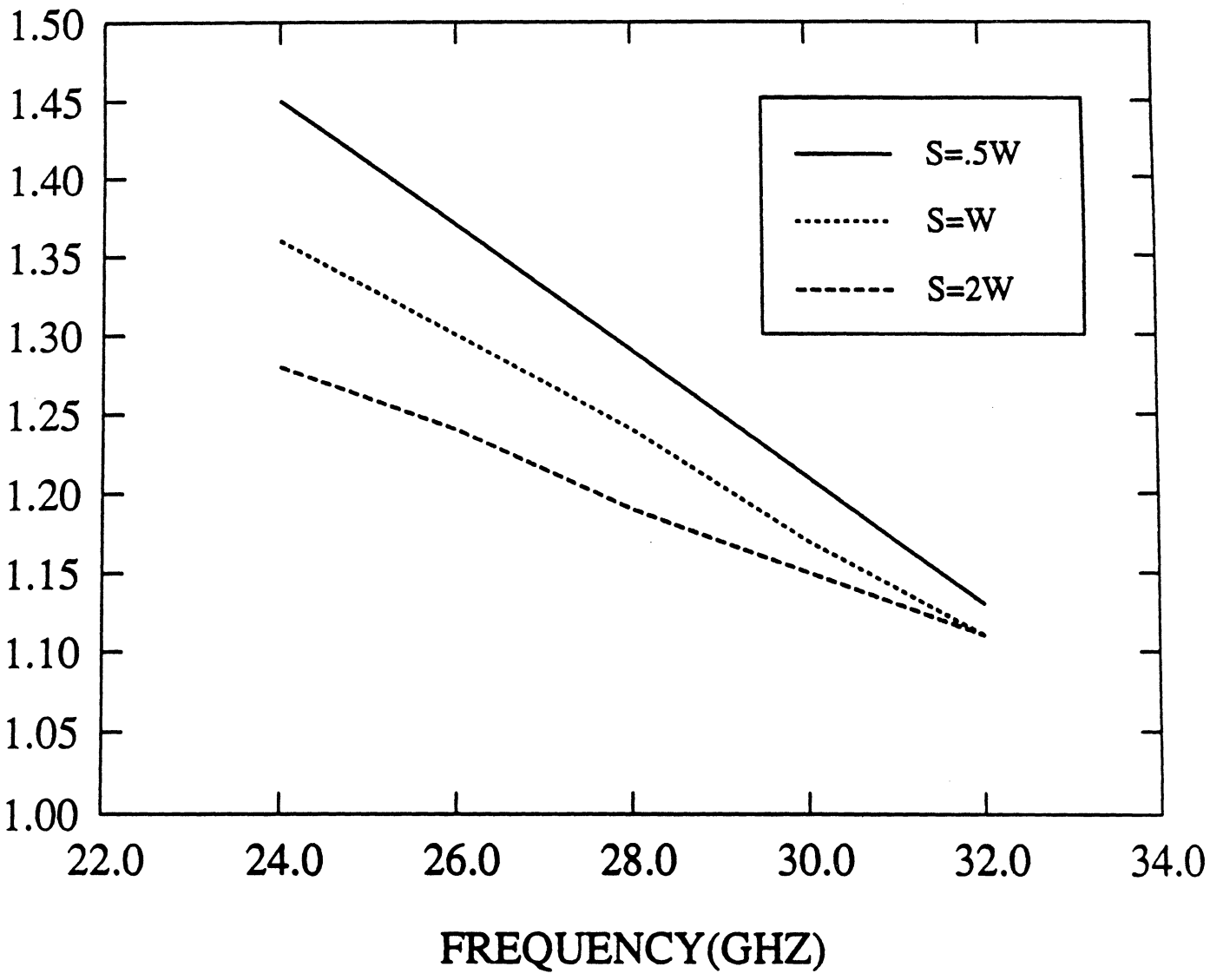

Figure 8: Phase Velocity in Meander Line

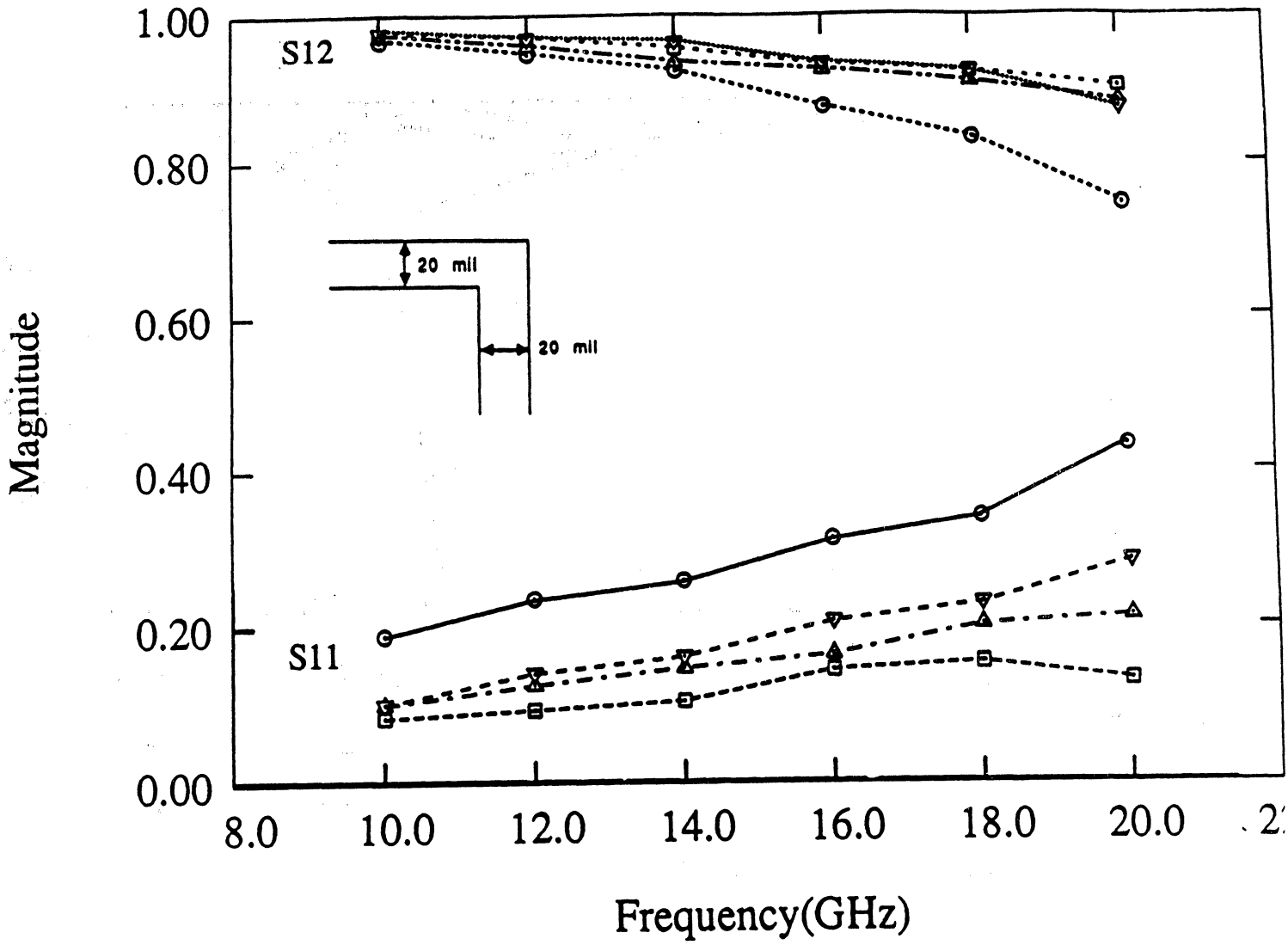

⊙	A
⊡	B
△	C
▽	D

Case	ϵ_{r1}	ϵ_{r2}	$h_1(mil)$	$h_2(mil)$
A	10.2		40	0
B	2.2		40	0
C	2.2	10.2	20	20
D	10.2	2.2	20	20

Figure 9: Scattering Parameters For Multilayer Microstrip Corner, W1=W2=20 mil

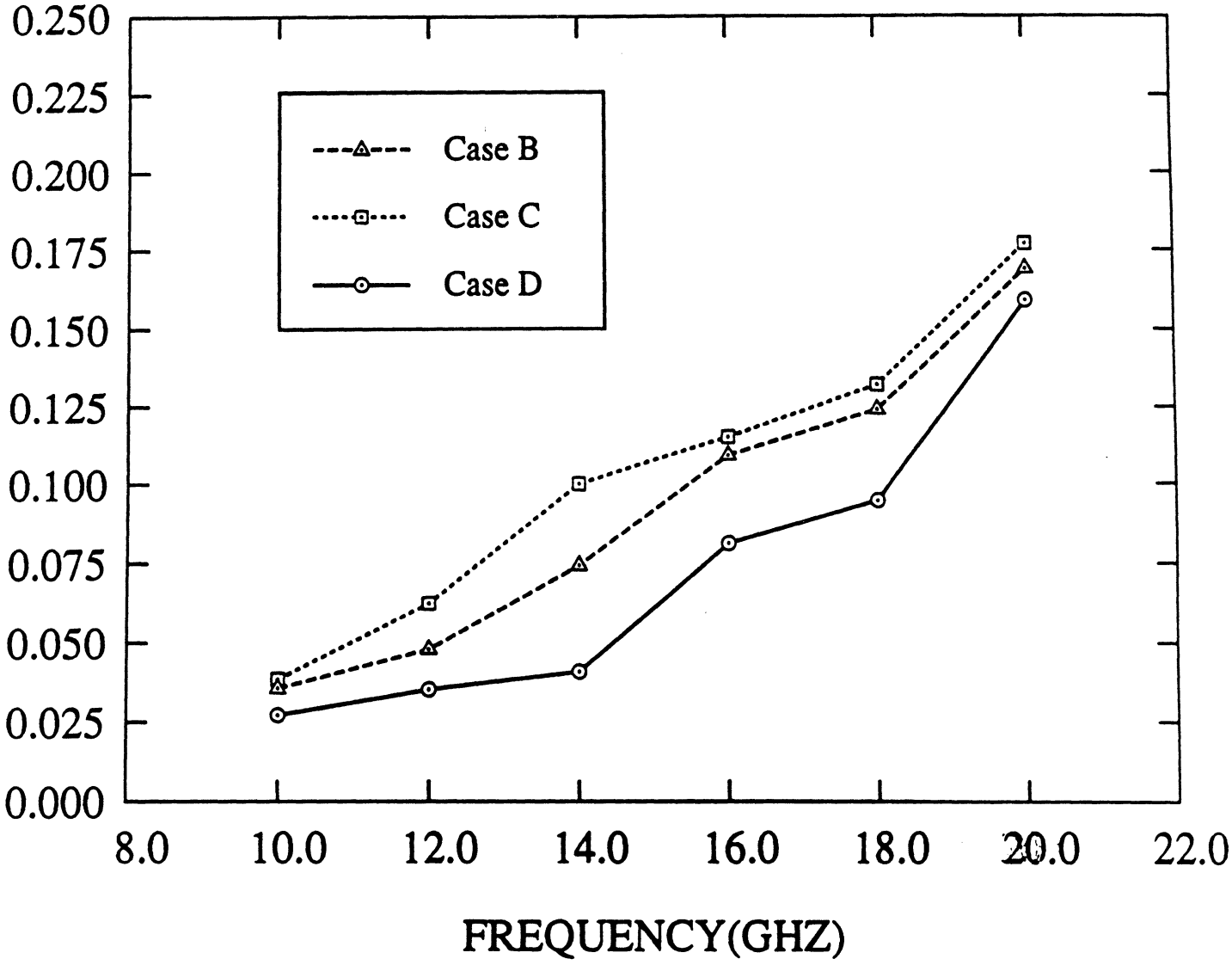

Figure 10: Radiation From Multilayer Microstrip Corner W1=W2=20 mil

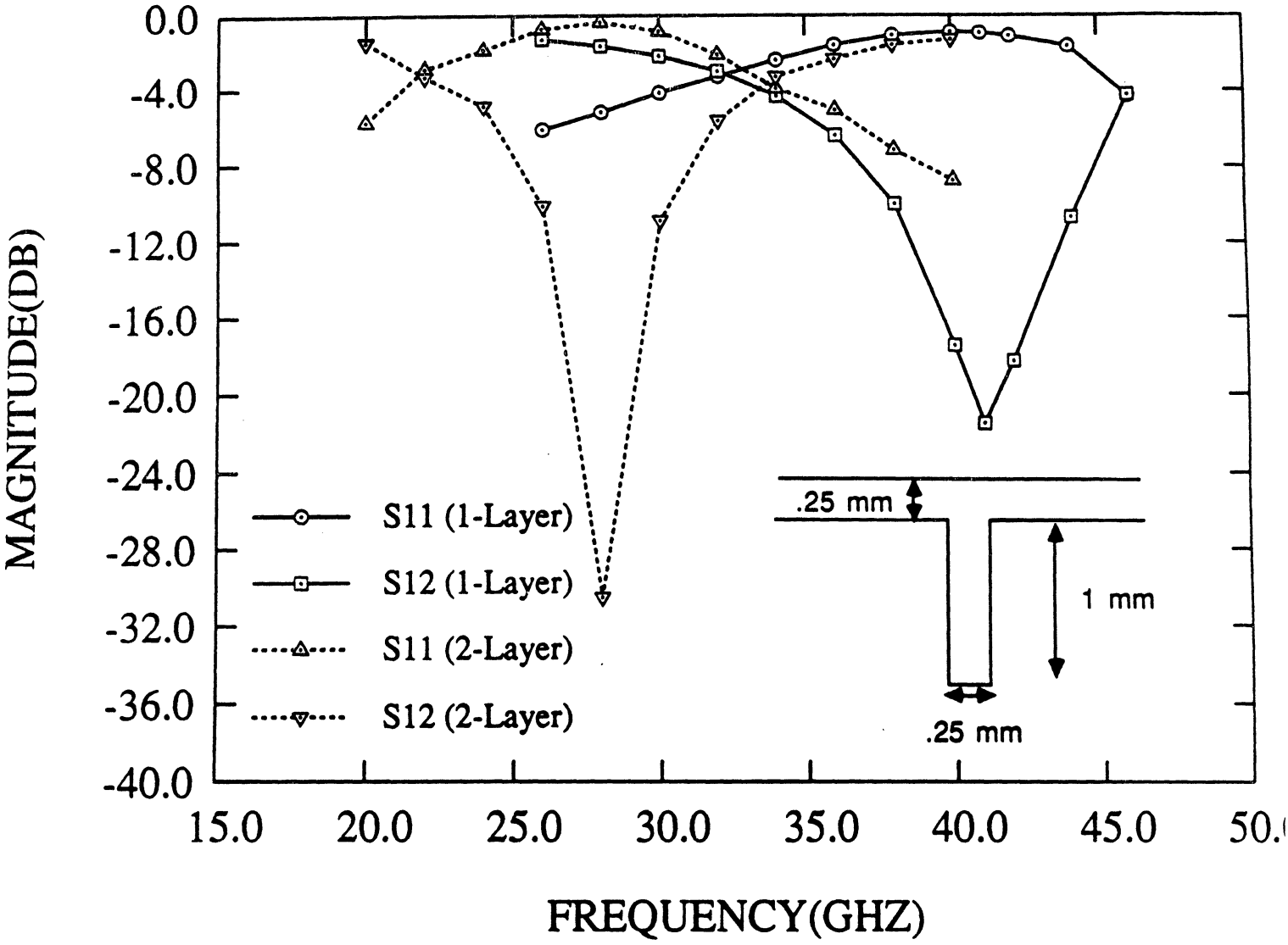

Figure 11: Scattering Parameters For Multilayer Microstrip Stub, W1=W2=.25mm,L=1 mm

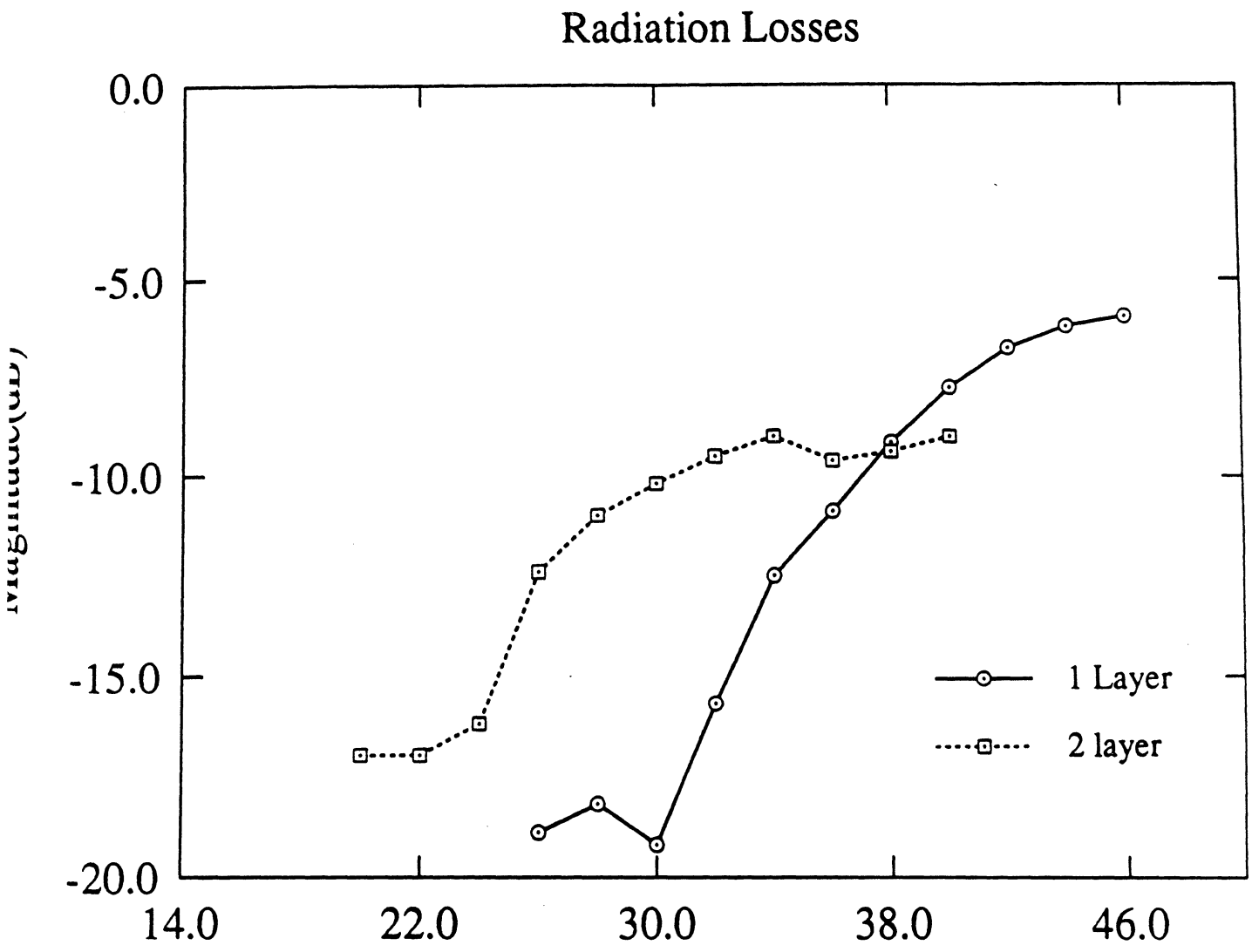

Figure 12: Radiation From Multilayer Microstrip Stub, W1=W2=.25mm,L=1 mm

AN INTEGRAL EQUATION METHOD FOR THE EVALUATION OF CONDUCTOR AND DIELECTRIC LOSSES IN HIGH FREQUENCY INTERCONNECTS

T.E. van Deventer*, P.B. Katehi* and A.C. Cangellaris**

*Radiation Laboratory
Department of Electrical Engineering and Computer Science
The University of Michigan
Ann Arbor, MI 48109-2122
**Electromagnetics Laboratory
Electrical and Computer Engineering Department
University of Arizona
Tucson, AZ 85721

Submitted to IEEE Transactions on Microwave Theory and Techniques

July 1989

List of Figures

Abstract-

An integral equation method is developed to solve for the complex propagation constant in multi-layered planar structures with arbitrary number of strip conductors on different levels. Both dielectric losses in the substrate layers and conductor losses in the strips and ground plane are considered. The Green's function included in the integral equation is derived by using a generalized impedance boundary formulation. The microstrip ohmic losses are evaluated by using an equivalent frequency-dependent impedance surface which is derived by solving for the fields inside the conductors. This impedance surface replaces the conducting strips and takes into account the thickness and skin effect of the strips at high frequencies. The effect of various parameters such as frequency, thickness of the lines and substrate surface roughness on the complex propagation constant are investigated. Results are presented for single strips, coupled lines and two-level interconnects. Good agreement with available literature data is shown.

1 Introduction

Shielded microstrip lines are widely used in microwave integrated circuits where they perform a great variety of functions. It is therefore very important to have an accurate knowledge of their characteristics, i.e. phase velocity, characteristic impedance and losses as a function of geometry and frequency. Because dissipative losses impose a major limitation on the performance of microstrip interconnects, passive circuits and radiating elements, it is of interest to improve loss analysis, whereby effects of substrate and non-perfectly conducting strips can be treated in-

dividually. Ohmic losses due to the finite conductivity of the strips is the prevalent loss effect at microwave and millimeter wave frequencies, and have been studied by several authors during the past fifty years but have been limited to lower frequencies and electrically thick strips.

The *incremental-inductance rule* derived by Wheeler [1] is the foundation for calculating the surface resistivity of conductive strips. From the knowledge of the resistivity, attenuation due to conductor losses has been evaluated by analytic [2], [3] and numerical [4] differentiation. The perturbation method is also frequently used in quasi-static techniques such as the boundary-element method [5], the finite-element method [6] as well as in spectral domain fullwave analyses [7], [8].

These techniques are strictly limited to electrically thick conducting strips, i.e. they assume that the conductors have a thickness much greater than the skin depth at the frequency of interest. The thickness is usually taken into account by a modification of the strip width [4], [9]. However in monolithic microwave and millimeter wave integrated circuits, where the metallization thickness is of the order of a few μm, the skin effect becomes an important issue. In the past few years, several researchers have studied the above problem using variational formulations [10], [11].

This paper represents an approach which evaluates losses in interconnects printed on multilayer substrates and surrounded by a shielding cavity. The electromagnetic fields are expressed by an integral equation which is solved independently inside the conducting strips and in the surrounding region. The solution for the fields inside the conductors provide the surrounding region with a relation between tangential

electric and magnetic fields on the surface of the strips which serves as an additional boundary condition. This boundary condition is satisfied by an equivalent infinitesimally thin impedance surface which then replaces the lossy conducting strips. The fields in the dielectric region, which consists of an arbitrary number of layers, are computed by a method of moments solution of Pocklington's integral equation subject to the new introduced boundary condition. The present technique is applied to several structures and a number of parameters are investigated.

2 Theory

Consider an infinitely long inhomogeneously-filled waveguide, with several microstrip lines on different levels within a multilayered configuration as shown in Figure 1. The conductor strips are assumed to have finite conductivity σ and thickness t. The conductor thickness is usually small compared to the strip dimensions, however this need not be the case, especially in monolithic microwave and millimeter wave integrated circuits on GaAs. Also, in practical circuits the strips are usually at least two widths away from the side walls of the waveguide to avoid coupling, therefore losses due to finite conductivity of these walls are neglected in this derivation. However, the effect of a lossy ground plane is analyzed. Both conducting and dielectric regions are assumed to be nonmagnetic with free-space permeability μ_0. Dielectric losses are accounted for by assuming a complex permittivity for each layer which in turn implies that the propagation constant $\gamma_z \equiv jk_z$ is a complex quantity. In the two-dimensional problem, each microstrip mode propagates rectilinearly along the z-direction with a dependence of the form

$e^{j(\omega t - k_z z)}$.

The integral equation formulation presented in this section is twofold. First, in the dielectric region, the problem is solved by a rigorous hybrid mode solution where an integral eigenvalue equation is set up. The Green's function is derived by using an equivalent transmission line for the representation of the fields along the direction normal to the dielectric interfaces. This formulation allows for multiple conductors on different planar levels.

Next, the field behavior inside the conductor is described by a quasi-TEM analysis where the magnetic vector potential is related to the unknown current distribution by a static Green's function. This method allows for the computation of the per unit length resistance $R(f)$ and the per unit length internal inductance of the strip $L_{in}(f)$ as function of frequency. An equivalent surface impedance is then defined which describes, in a physical equivalent sense, the frequency-dependent field penetration in the lossy strips.

The novelty of this method resides in the application of the boundary condition on the strip where the tangential electric field is related to the finite current on the strip by the surface impedance described above. The resulting general integral equation that accounts for both dielectric and conductor losses is solved numerically by the method of moments.

2.1 Integral Equation Formulation in the Dielectric Region

The electric field excited by an electric current source depends upon the surface current density $\bar{J}$ as follows

$$\bar{E}(\bar{r}) = \int\int \bar{\bar{G}}(\bar{r}/\bar{r}') \cdot \bar{J}(\bar{r}')\, ds' \tag{1}$$

where $\bar{\bar{G}}$ represents the dyadic Green's function in the dielectric regions. The Green's function is derived by evaluating the electric field due to a two-dimensional infinitesimal current source $\bar{J}(\bar{r}') = (\hat{y} + \hat{z})\,\delta(\bar{r} - \bar{r}')$, where $\bar{r}'$ is the position vector of the source. Because of the existence of air and dielectric interfaces, shielded microstrip lines propagate hybrid modes. Determination of these hybrid fields is facilitated by the use of magnetic and electric vector potentials having components in the direction perpendicular to the interfaces, i.e. the x-direction [12], [13].

For the case of two-dimensional interconnects, the problem is uniform in the z-direction and the Green's function can therefore be solved in the transformed k_z-space. The spectral dyadic Green's function $\bar{\bar{\bar{G}}}$ is obtained by solving the boundary-value problem of the structure under study [14].

In the present derivation, for sake of clarity, the simple geometry illustrated in Figure 2 is studied. However, the Green's function is formulated in a generalized way, which can be applied to more complicated problems. The equivalent structure containing impedance boundaries is shown in Figure 2(b) , where the current is displaced from the interface to generalize the problem and to ease the application of the boundary conditions. The impedance boundaries on the upper and lower interfaces are determined by the use of a single transmission line problem. This

formalism has been applied extensively in the past to open structures [15]. The boundary conditions at the upper ($i = 1$) and lower ($i = 2$) interfaces can be solved separately for LSE (subscript a) and LSM (subscript f) modes. The impedance $\eta^i_{a,f}$ is equivalent to the impedance of a transmission line terminated by a load impedance $Z^{a,f}_{Li}$ with characteristic impedance $Z^{a,f}_{oi}$. The load impedance $Z^{a,f}_{Li}$ may be a lumped impedance, such as the surface resistance of the ground plane, as suggested in Figure 2(b), or it may be the impedance presented by another substrate layer. The characteristic impedance $Z^{a,f}_{oi}$ is given by the appropriate TM and TE wave impedances.

Inside the equivalent structure, the homogeneous scalar wave equations for A_x and F_x have to be solved in regions (1) ($x > x'$) and (2) ($x < x'$). Applying the method of separation of variables, the following boundary conditions need to be satisfied: (i) vanishing electric fields on the side walls, (ii) impedance boundaries on the upper and lower walls as

$$\left(\frac{\tilde{E}_y}{\tilde{H}_z}\right)^i_{a,f} = \eta^i_{a,f}, \tag{2}$$

(iii) continuity of the electric fields at $x = x'$, and (iv) discontinuity of the magnetic field components due to the infinitesimal two-dimensional current source at $x = x'$

$$\hat{n} \times (\tilde{\vec{H}}^{(1)} - \tilde{\vec{H}}^{(2)}) = (\hat{y} + \hat{z})\, \delta(y - y') e^{jk_z z'}|_{x=x'}. \tag{3}$$

Because the current sources are assumed to have both longitudinal and transverse components, four out of six components of the dyadic Green's function are needed.

A more general current distribution $\bar{J}$ may be written in the form

$$\bar{J}(\bar{r}') = \delta(x - x')\,\bar{j}(y')\,e^{-jk_z^{MS}z'} \tag{4}$$

where k_z^{MS} is the unknown propagation constant of the microstrip. In view of (4), the integral equation for the electric field (1) can be expressed as

$$\bar{E}(\bar{r}) \;=\; \int\int_S \bar{\bar{g}}(x,y/x',y')\,e^{-jk_z(z-z')} \;\cdot\; \bar{j}(y')\,e^{-jk_z^{MS}z'}\,dy'\,dz' \tag{5}$$

where S is the surface of the strip conductors. In the above, the z-dependence of both the Green's function and the current is shown explicitly.

Introducing the spectral form of the Green's function $\tilde{\bar{\bar{g}}}$, and using the sifting property of the Fourier transform, the electric field can be evaluated at any transverse cross-section as

$$\bar{E} \;=\; \int_{C_w} \tilde{\bar{\bar{g}}}(x,y/x',y') \cdot \bar{j}(y')\,dy' \;|_{k_z=k_z^{MS}} \tag{6}$$

where C_w is a path along the width of the conductor [14].

The above expression satisfies all boundary conditions except the ones on the surface of the strip conductors. For perfectly conducting strips we enforce the Dirichlet condition of vanishing tangential electric field on the surface of the line. This boundary condition is applied to (6) which will be satisfied for discrete values of k_z^{MS} corresponding to the dominant and possibly higher-order modes propagating in the structure. For the general case of strips with finite thickness and finite conductivity this condition is not applicable anymore. Indeed, due to the finite conductivity, the fields penetrate inside the strips. An exact analysis of this case requires Maxwell's equations to be solved throughout the entire domain, i.e., in the

dielectric regions and inside the lossy strips. Such an analysis is very involved and will not be undertaken here. Instead, we shall follow an alternative, approximate method based on an equivalent representation of the lossy strips by impedance surfaces. These equivalent surfaces are characterized by frequency-dependent surface impedances which are derived from a quasi-TEM analysis of the field penetration and the resulting current distributions inside the lossy strips. The derivation of these impedances is discussed next.

2.2 Derivation of the Equivalent Surface Impedance

Under the assumption that the transverse component of the current is negligible compared to the longitudinal component, this method is valid through the millimeter wave frequency range. In this study the current density in the lossy strips of Figure 1 has the longitudinal component only. An integral equation formulation for the frequency-dependent current distributions in the lossy strips is then possible. The derivation of the pertinent integral equation along with its numerical solution have been presented in [16], [17] and will not be repeated here. Figure 3 illustrates the results of this formulation by showing the magnitude of the current density along the width of the strip, plotted for four different distances s_1, s_2, s_3 and s_4 from the bottom side of the strip.

Once the current distributions have been computed, the per unit length resistance $R(f)$ and inductance $L(f)$ of the lossy strips can be found from energy considerations as described in [17]. The per unit length internal inductance of the strip is then computed as

$$L_{in}(f) = L(f) - L_{\infty}, \tag{7}$$

where L_∞ is the per unit length inductance of the strip in the limit $\sigma \rightarrow \infty$, in which case the current flows on the surface of the strip and there is no field penetration. Knowledge of the per unit length strip resistance and internal inductance allows us to express the per unit length voltage drop ΔV along the lossy strip as

$$-\Delta V = [R(f) + j2\pi f L_{in}(f)]\, I \qquad (V/m) \tag{8}$$

where I is the total current flowing in the strip.

In order to derive the desirable surface impedance we start with the standard definition for the surface impedance of an imperfect conductor as the ratio of the tangential component of the electric field to the surface current density at the conductor surface

$$E_z(\tau) = Z(\tau) J_{zs}(\tau) = Z(\tau) H_y(\tau), \tag{9}$$

where τ is the transverse coordinate along the surface of the conductor. Integrating (9) along the side of the strip we have

$$\int_0^W E_z(\tau) d\tau = \int_0^W Z(\tau) H_y(\tau) d\tau, \tag{10}$$

where W is the width of the strip. From (10) using the mean value theorem for Riemann integration [18] we can write

$$\int_0^W E_z(\tau) d\tau = Z(\tau_0) \int_0^W H_y(\tau) d\tau, \tag{11}$$

where $\tau_0 \in [0, W]$. Dividing both sides of (11) by W and recognizing the integral on the right-hand side as the total current flowing on the surface we can write

$$\tilde{E}_z = Z(\tau_0)\, \frac{I}{W}, \tag{12}$$

where $\tilde{E}_z$ is the average value of the longitudinal component of the electric field on the strip. Obviously, this value can be thought of as the negative of the per unit length average voltage drop along the strip, in which case (8) and (12) lead to the relation

$$Z(\tau_o) = W\,[R(f) + j\omega L_{in}(f)]. \tag{13}$$

This is the desirable expression for the surface impedance of the equivalent impedance surface to be used in place of the lossy strip. In what follows, we shall denote this surface impedance as $Z_l(f)$ where the subscript l suggests its relation to the longitudinal current on the strip. A transverse component of the current also exists, and a transverse surface impedance Z_t can be defined as discussed in the following section.

2.3 Application of Boundary Condition

The electric and magnetic fields tangential to the surface of the strips are related through the surface impedance derived in the previous section as

$$\frac{E_z}{H_y} \equiv Z_l(f). \tag{14}$$

For most practical purposes, the dominant part of the conductor loss is due to the longitudinal component of the current, for which the accurate longitudinal surface impedance $Z_l(f)$ has been proposed. However, as the frequency of interest becomes higher and/or the width of the strip increases, the transverse component of the current becomes more significant and needs to be accounted for. This is being done using the standard surface impedance for an infinite resistive plane as

$$-\frac{E_y}{H_z} \equiv Z_t = (1+j)\frac{1}{\sigma\delta}, \tag{15}$$

where σ is the conductivity of the strip and δ the skin depth at the frequency of interest. Even if the width of the strip is finite, use of (15) is justified by the fact that the strip is assumed to be infinite in the direction perpendicular to the flow of the transverse component of the current.

In view of (14) and (15), equation (6) takes the form

$$\bar{E} = \int_{C_w} \bar{\bar{\bar{g}}}(x, y/x', y') \cdot \bar{j}(y')\, dy' + \bar{\bar{Z}} \cdot (\bar{H} \times \hat{n})\,|_{k_z = k_z^{MS}} \tag{16}$$

where $\bar{\bar{Z}}$ is a dyadic quantity that we call *the dyadic surface impedance* and is given by

$$\bar{\bar{Z}} = Z_t \hat{y}\hat{y} + Z_l \hat{z}\hat{z}. \tag{17}$$

Recognizing the boundary condition for the magnetic field as

$$\hat{n} \times \bar{H} = \bar{J} \tag{18}$$

equation (16) becomes

$$\int_{C_w} \bar{\bar{\bar{g}}}(x, y/x', y') \cdot \bar{j}(y')\, dy' - \bar{\bar{Z}} \cdot \bar{j}(y')\,|_{k_z = k_z^{MS}} = 0 \tag{19}$$

The method of moments is adopted here to solve for the current distribution. The two-dimensional surface current may be written as

$$\bar{j}(y') = j_y(y')\hat{y} + j_z(y')\hat{z} \tag{20}$$

where $j_y(y')$ and $j_z(y')$ are unknown functions of y'. Entire domain basis functions are chosen to approximate the behavior of the current distribution. The longitudinal current is represented by Chebychev polynomials of the first kind T_i, and the transverse current is approximated by Chebychev polynomials of the second kind

U_i. These basis functions are multiplied by their respective weighting functions in order to satisfy the edge conditions

$$j_y(y') = \sum_{p=1}^{P} I_{yp}\, U_p\left(\frac{2}{W}(y'-y_0)\right)\sqrt{1-\left(\frac{2}{W}(y'-y_0)^2\right)} \tag{21}$$

$$j_z(y') = \sum_{q=0}^{P-1} I_{zq}\,\frac{T_q(\frac{2}{W}(y'-y_0))}{\sqrt{1-(\frac{2}{W}(y'-y_0)^2)}}. \tag{22}$$

In the above expressions W is the width of the strip and y_0 the distance from the origin to the center of the strip. Introducing these expressions for the basis functions, equation (19) results in closed-form integrals that simplify to Bessel functions of integer order.

The testing functions are chosen as Chebychev polynomials of the form

$$w_p^y(y) = U_p\left(\frac{2}{W}(y-y_0)\right) \tag{23}$$

$$w_q^z(y) = T_q\left(\frac{2}{W}(y-y_0)\right). \tag{24}$$

This method is a variation of Galerkin's procedure. The integrals resulting from the weighted averages are expressed in terms of spherical Bessel functions. This technique results in a homogeneous system of simultaneous algebraic equations which can be solved by setting the determinant of the impedance matrix $[\mathcal{Z}]$ equal to zero. Expressions for the elements of $[\mathcal{Z}]$ are given in the Appendix. The roots of the determinant correspond to the propagation constants of the excited modes.

3 Numerical Results

Based on the theory presented in the previous section, the complex propagation constant in high frequency interconnects is evaluated as a function of various

parameters by using Muller's algorithm with deflation. Each element of this matrix involves a summation over the modes of the inhomogeneously filled waveguide along the y-direction. The number of modes considered is enough to insure convergence.

As it has been discussed by many authors, isolated microstrip interconnects can propagate a dominant mode with zero cut-off frequency and higher order modes which are in one-to-one correspondence with the modes of the inhomogeneously filled waveguide surrounding them. All these modes are hybrid in nature and exhibit strong dependence on the electrical and geometrical characteristics of the microstrip interconnects and the shielding structure. From the parameters which affect the characteristics of the propagating modes, the strip width W to substrate thickness ratio (aspect ratio) and the operating frequency are the most important ones. This paper gives an extensive parametric study of the attenuation of the dominant mode and the derived results are compared with available data whenever possible.

In Figure 4, conductor and dielectric losses calculated with the present technique are shown as a function of the aspect ratio. For thick strips, results derived in this paper are compared with the finite element method (FEM) [6], the spectral domain method (SDM) [7], [19] and an analytic differentiation of Wheeler's *incremental inductance rule* [2] [1]. All the existing full-wave analysis models evaluate conductor losses by using a perturbation method where the surface resistivity is given by the *incremental inductance rule* and, as a result, cannot predict losses for conducting

[1] This analytic differentiation is implemented through the microwave CAD software package *LineCalc* available from EESOF.

strips with thickness of the order of a skin depth. The effect of the conductor strip thickness on conductor losses is explicitly shown on Figure 5. On the figure, conductor losses versus aspect ratio are plotted for the case of $t = 0.5\delta$ which appear substantially different from the case of $t = 2, 3$ and 4δ (= electrically thick strips). Our results correctly predict that as the thickness of the strip increases to values large compared to the skin depth, the loss decreases significantly to the thick strip limit. This, of course, is due to the fact that the current is forced to flow through a smaller area.

The skin-effect problem may also be described as a function of frequency. The attenuation constant α is plotted in Figure 6 for frequencies up to 20 GHz. Also shown are the equivalent surface resistance of the strip (13) and the surface resistivity R_s of the infinite thick plane representing the ground plane resistance. By using R_s as the surface resistivity of the ground plane, results have been derived which show the effect of the lossy ground on conductor losses (see Figure 7). This effect is very important and therefore losses due to ground plane cannot be neglected.

The present method also allows to account accurately for multiple metallizations and roughness of the surface of the strip conductors. In Figure 8, the effect of a periodic variation of the surface roughness on conductor losses is plotted as a function of frequency.

The technique presented in this paper has also been applied to evaluate conductor and dielectric losses for the even and odd excitation modes in the case of two edge-coupled electrically thick strips. The derived results are plotted in Figure 9

as a function of the separation between the two strips and are compared to results derived with the spectral domain method [7], [19]. The agreement is very good. Similar results are presented in Figure 10 for the case of two-level interconnects as a function of frequency.

4 Summary

An integral equation method has been applied to calculate the propagation constant in shielded multi-layered structures involving an arbitrary number of non-perfectly conducting strips by using the combination of a static Green's function inside the strips and a hybrid Green's function formulation in the dielectrics. This method allows for the evaluation of dielectric losses in the substrate layers and conductor losses in strips of arbitrary thickness. The skin-effect problem is adressed and results show an increase in the attenuation constant for thin strips. As expected, finite conductive ground plane and roughness of the strip increase the attenuation constant substantially. Several interconnects structures are analysed, such as single lines, edge-coupled and broadside-coupled strips and compare well with available data.

5 Acknowledgements

This work was supported by the Army Research Office under contract project DAAL03-K-0088(23836-EL) (University of Michigan) and by the Semiconductor Research Corporation under contract number 88-MP-086 (University of Arizona).

6 Appendix

Expressions for the elements of the impedance matrix $\mathcal{Z}$

$$\left(\mathcal{Z}_{yy}^{qp}\right)^i = \frac{2}{b} j\omega\mu_0 \sum_m -\frac{1}{k_y^2+k_z^2}\left\{\frac{k_z^2}{k_{xr}}\left(\varphi_m^f\right)^i + \frac{k_y^2\,k_{xr}}{k_r^2}\left(\varphi_m^a\right)^i\right\} \mathcal{I}_q^{(4)}\mathcal{I}_p^{(2)} - Z_t\mathcal{I}_{qp}^{(6)} \quad (25)$$

$$\left(\mathcal{Z}_{yz}^{qp}\right)^i = \frac{2}{b}\omega\mu_0 \sum_m \frac{k_y\,k_z}{k_y^2+k_z^2}\left\{-\frac{1}{k_{xr}}\left(\varphi_m^f\right)^i + \frac{k_{xr}}{k_r^2}\left(\varphi_m^a\right)^i\right\} \mathcal{I}_q^{(4)}\mathcal{I}_p^{(1)} \quad (26)$$

$$\left(\mathcal{Z}_{zy}^{qp}\right)^i = \frac{2}{b}\omega\mu_0 \sum_m \frac{k_y\,k_z}{k_y^2+k_z^2}\left\{-\frac{1}{k_{xr}}\left(\varphi_m^f\right)^i + \frac{k_{xr}}{k_r^2}\left(\varphi_m^a\right)^i\right\} \mathcal{I}_q^{(3)}\mathcal{I}_p^{(2)} \quad (27)$$

$$\left(\mathcal{Z}_{zz}^{qp}\right)^i = \frac{2}{b} j\omega\mu_0 \sum_m \frac{1}{k_y^2+k_z^2}\left\{\frac{k_y^2}{k_{xr}}\left(\varphi_m^f\right)^i + \frac{k_z^2\,k_{xr}}{k_r^2}\left(\varphi_m^a\right)^i\right\} \mathcal{I}_q^{(3)}\mathcal{I}_p^{(1)} - Z_l\mathcal{I}_{qp}^{(5)} \quad (28)$$

where

$$k_r = \omega\sqrt{\epsilon_r^*\mu_0} \quad (29)$$

$$k_y = \frac{m\pi}{b} \quad (30)$$

$$k_{x_r} = \sqrt{(k_r)^2 - k_y^2 - k_z^2} \quad (31)$$

and

$$\left(\varphi_m^{a,f}\right)^1 = -\frac{\frac{\cos k_{xr}(x-h)}{\cos k_{xr}(x'-h)}\,\frac{\tan k_{xr}(x-h)+j\eta_{a,f}^1}{1-j\eta_{a,f}^2\tan k_{xr}x'}}{\frac{\tan k_{xr}(x'-h)+j\eta_{a,f}^1}{\tan k_{xr}x'+j\eta_{a,f}^2} - \frac{1-j\eta_{a,f}^1\tan k_{xr}(x'-h)}{1-j\eta_{a,f}^2\tan k_{xr}x'}} \quad (32)$$

$$\left(\varphi_m^{a,f}\right)^2 = \frac{\frac{\cos k_{xr}x}{\cos k_{xr}x'}\,\frac{\tan k_{xr}x+j\eta_{a,f}^2}{1-j\eta_{a,f}^1\tan k_{xr}(x'-h)}}{\frac{\tan k_{xr}x'+j\eta_{a,f}^2}{\tan k_{xr}(x'-h)+j\eta_{a,f}^1} - \frac{1-j\eta_{a,f}^2\tan k_{xr}x'}{1-j\eta_{a,f}^1\tan k_{xr}(x'-h)}}. \quad (33)$$

In (29), ϵ_r^* is the complex permittivity of the substrate, and i $(= 1, 2)$ represents the regions above and below the point source, respectively.

Further definitions necessary for the interpretation of (25)-(28) are provided as

$$\mathcal{I}_n^{(1)} = \frac{W}{2}\,\pi\,\sin(k_y y_0 + n\frac{\pi}{2})\,J_n(k_y\frac{W}{2}) \quad (34)$$

$$\mathcal{I}_n^{(2)} = \frac{\pi}{k_y}\,(n+1)\cos(k_y y_0 + n\frac{\pi}{2})\,J_{n+1}(k_y\frac{W}{2}) \quad (35)$$

$$\mathcal{I}^{(5)} = \begin{cases} W\frac{\pi}{2} & \text{, for m = n = 0} \\ W\frac{\pi}{4} & \text{, for m = n} \neq 0 \\ 0 & \text{, for m} \neq \text{n} \end{cases} \tag{36}$$

and

$$\mathcal{I}^{(6)} = \begin{cases} W\frac{\pi}{4} & \text{, for m = n} \\ 0 & \text{, for m} \neq \text{n.} \end{cases} \tag{37}$$

No general recurrence formulas were found for $\mathcal{I}^{(3)}$ and $\mathcal{I}^{(4)}$. However, these integrals can be written in a simple form as a weighted sum of spherical Bessel functions.

In equations (32) and (33), η_a^i and η_f^i are given by

$$\eta_a^i = \frac{\omega\epsilon_r^*}{k_{x_r}} Z_{0i}^a \frac{Z_{Li}^a + jZ_{0i}^a \tan k_{x_i}h_i}{Z_{0i}^a + jZ_{Li}^a \tan k_{x_i}h_i} \tag{38}$$

$$\eta_f^i = \frac{k_{x_r}}{\omega\mu_0} Z_{0i}^f \frac{Z_{Li}^f + jZ_{0i}^f \tan k_{x_i}h_i}{Z_{0i}^f + jZ_{Li}^f \tan k_{x_i}h_i}. \tag{39}$$

where

$$Z_{0i}^f = \frac{\omega\mu_0}{k_{x_i}} \tag{40}$$

$$Z_{0i}^a = \frac{k_{x_i}}{\omega\epsilon_i^*} \tag{41}$$

References

[1] H. A. Wheeler, "Formulas for the Skin Effect," *Proc. IRE*, vol. 30, pp 412-424, Sept. 1942.

[2] R. A. Pucel, D. J. Masse, C. P. Hartwig, "Losses in Microstrip," *IEEE Trans. Microwave Theory Tech.*, vol. MTT-16, No. 6, pp 342-350, June 1968.

[3] M.V. Schneider, " Microstrip Lines for Microwave Integrated Circuits," *The Bell System Technical Journal*, pp 1421-1444, May-June 1969.

[4] H. A. Wheeler, "Transmission-Line Properties of a Strip on a Dielectric Sheet on a Plane," *IEEE Trans. Microwave Theory Tech.*, vol. MTT-25, No. 8, pp 631-647, August 1977.

[5] B.E. Spielman, "Dissipation Loss Effects in Isolated and Coupled Transmission Lines," *IEEE Trans. Microwave Theory Tech.*, vol. MTT-25, No. 8, pp 648-655, August 1977.

[6] Z. Pantic-Tanner, R. Mittra, "Finite-Element Matrices for Loss Calculation in Quasi-TEM Analysis of Microwave Transmission Lines," *Microwave and Optical Technology Letters*, vol. 1, No. 4, pp 142-146, June 1988.

[7] D. Mirshekar-Syahkal, J. B. Davies, "Accurate Solution of Microstrip and Coplanar Structures for Dispersion and for Dielectric and Conductor Losses", *IEEE Trans. Microwave Theory Tech.*, vol. MTT-27, No. 7, pp 694-699, July 1979.

[8] C.M. Crowne, "Microstrip Conductor Losses Calculated by Full Wave and Perturbational Approaches," *Electronics Letters*, vol. 24, No. 9, pp 552-553, April 1988.

[9] R.H. Jansen, "High Speed Computation of Single and Coupled Microstrip Parameters Including Dispersion, High-Order Modes, Loss and Finite Strip Thickness", *IEEE Trans. Microwave Theory Tech.*, vol. MTT-26, No. 2, pp 75-82, February 1978.

[10] P. Waldow, I. Wolff, "The Skin-Effect at High Frequencies", *IEEE Trans. Microwave Theory Tech.*, vol. MTT-33, No. 10, pp 1076-1082, October 1985.

[11] G.I. Costache, "Finite Element Method Applied to Skin-Effect Problems in Strip Transmission Lines", *IEEE Trans. Microwave Theory Tech.*, vol. MTT-35, No. 11, pp 1009-1013, November 1987.

[12] N.K. Das, D.M. Pozar, "A Generalized Spectral-Domain Green's Function for Multilayer Dielectric Substrates with Application to Multilayer Transmission Lines", *IEEE Trans. Microwave Theory Tech.*, vol. MTT-35, No. 3, pp 326-335, March 1987.

[13] T.G. Livernois, P.B. Katehi, "A Generalized Method for Deriving the Space-Domain Green's Function in a Shielded, Multilayer Substrate Structure with Applications to MIS Slow-Wave Transmission Lines", *IEEE Trans. Microwave Theory Tech.*, accepted for publication.

[14] T.E. van Deventer and P.B. Katehi, "Conductor Losses in High Frequency Interconnects," Radiation Laboratory Report, University of Michigan, in preparation.

[15] L. Beyne, D. de Zutter, "Green's Function for Layered Lossy Media with Special Application to Microstrip Antennas," *IEEE Trans. Microwave Theory Tech.*, vol. MTT-36, No. 5, pp 875-881, May 1988.

[16] A.C. Cangellaris, "The Importance of Skin-Effect in Microstrip Lines at High Frequencies", *IEEE MTT-International Symposium Digest*, pp 197-198, May 1988.

[17] A.C. Cangellaris, J.L. Prince, O.A. Palusinski, "Modeling of High-Speed Interconnects; An Integral Equation Approach to Inductance Computation," *Proceedings of the 1988 Summer Computer Simulation Conference*, pp. 33-36, July 1988.

[18] E.T. Whittaker, G.N. Watson, *A Course of Modern Analysis*, Cambridge University Press, 1927, pp. 65-66.

[19] D. Mirshekar-Syahkal, "An Accurate Determination of Dielectric Loss Effect in Monolithic Microwave Integrated Circuits Including Microstrip and Coupled Microstrip Lines," *IEEE Trans. Microwave Theory Tech.*, vol. MTT-31, No. 11, pp 950-954, November 1983.

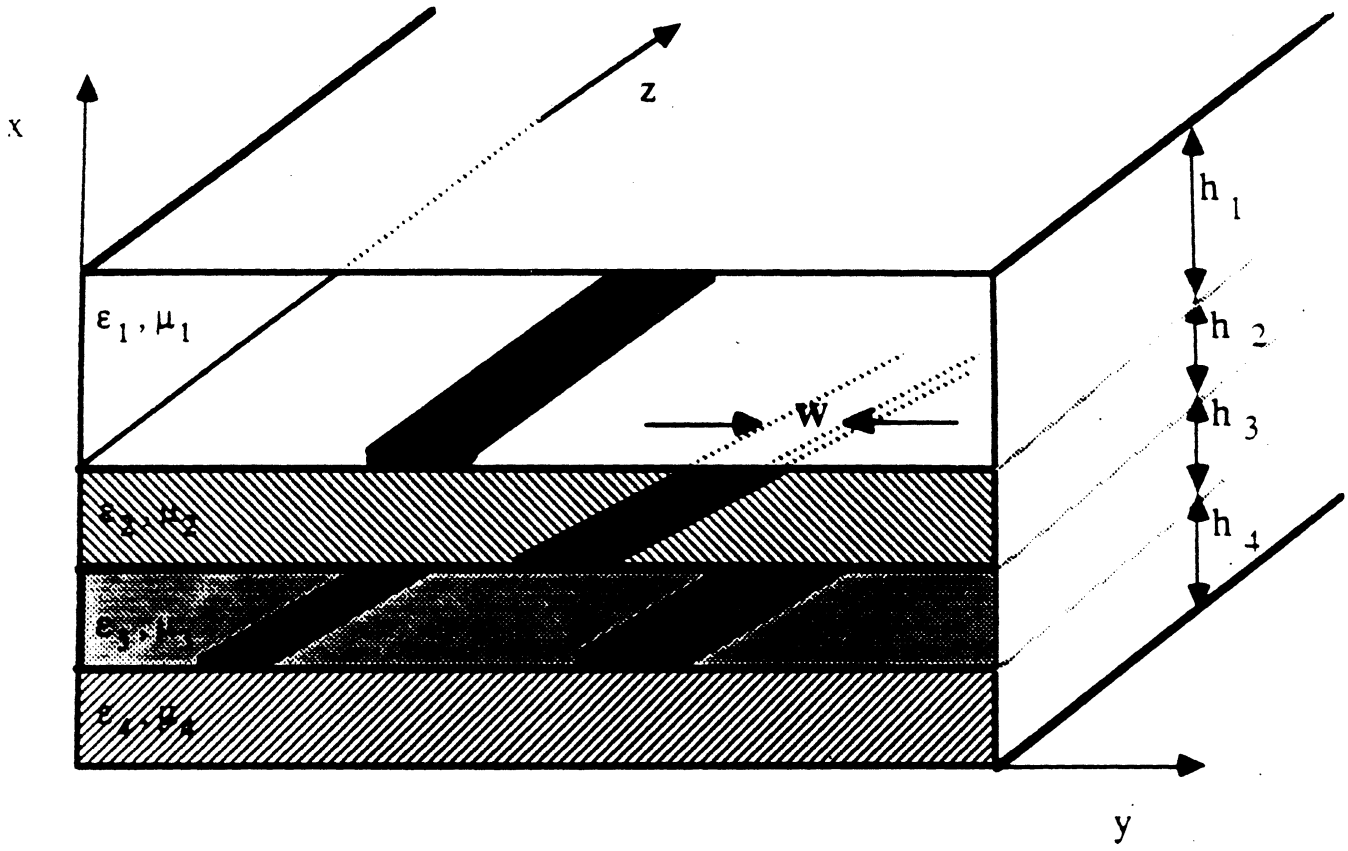

Figure 1: General Shielded Microstrip Configuration

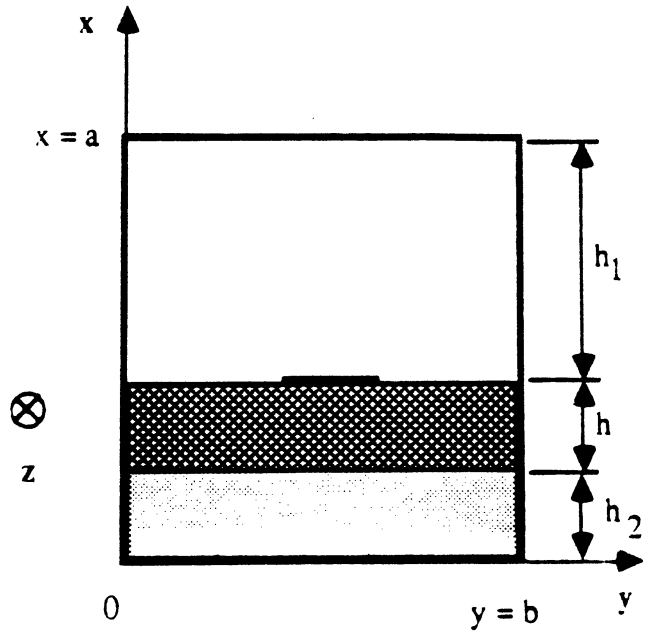

a. Generic cross-section of a single shielded line

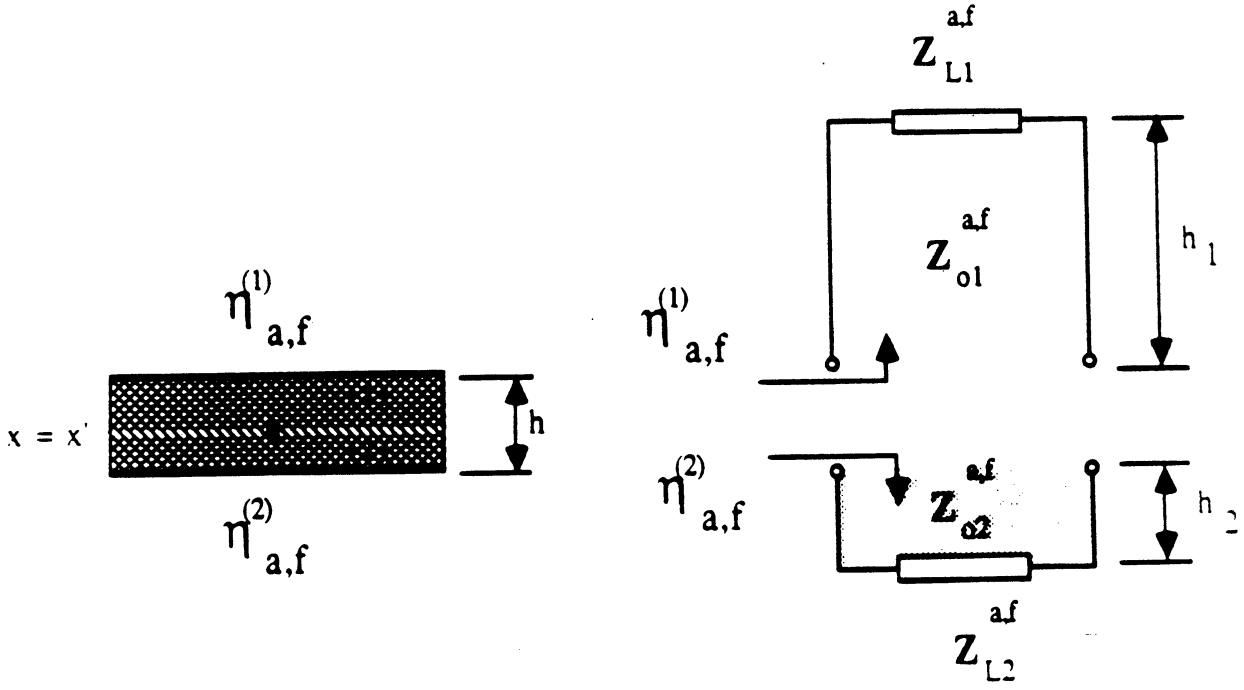

b. Equivalent geometry containing impedance boundaries

Figure 2: Multiple Layered Structure

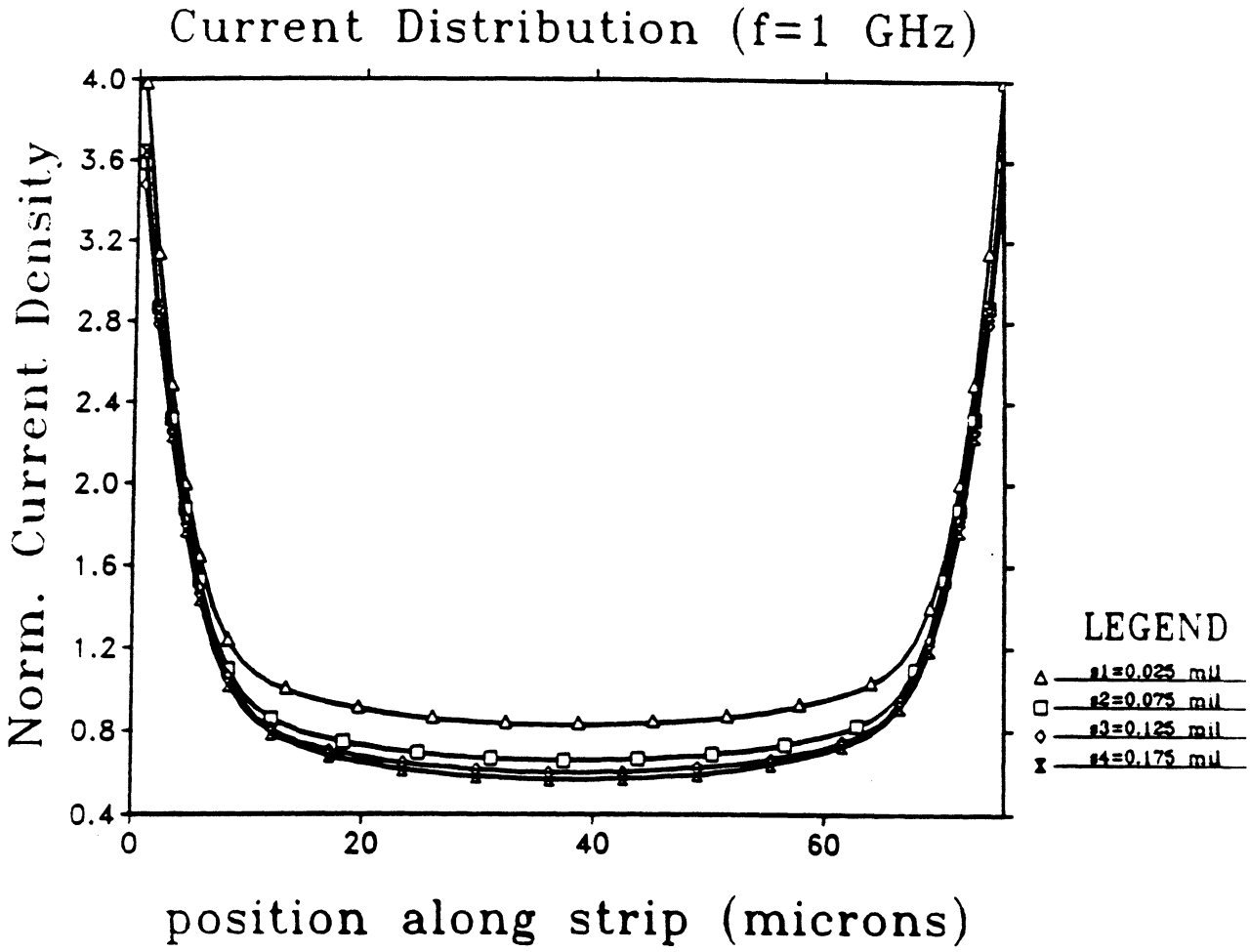

Figure 3: **Magnitude of current density inside a rectangular strip at a height of 3 mils above a perfectly conducting ground** (W = 3 mils, σ = 4 x 10^7 S/m, f = 1 GHz, t = 0.2 mils)

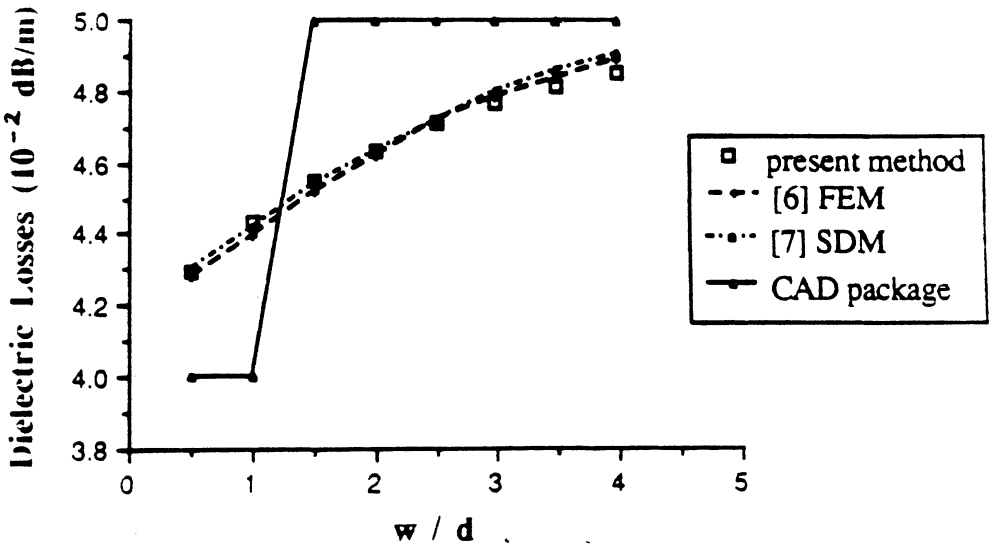

...ric attenuation as a function of w/d

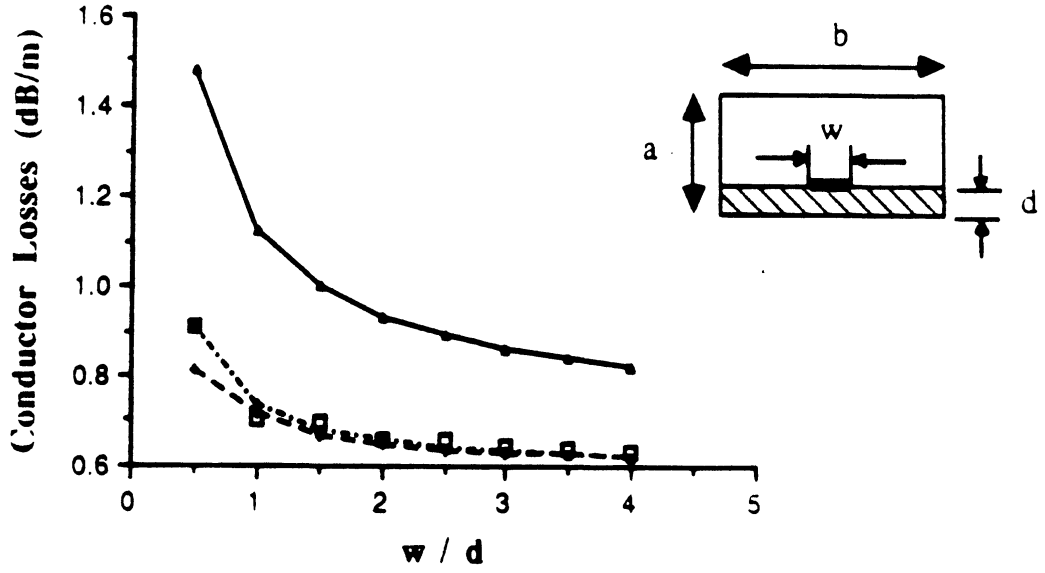

b. Ohmic attenuation as a function of w/d

Figure 4: Conductor and dielectric losses of a single strip versus strip width (a = 10 mm, b = 20 mm, d = 1mm, ϵ_r = 10, σ = 3.33 x 10^7 S/m, tanδ = 2 x 10^{-4}, f = 1 GHz, t = 0.01 mm)

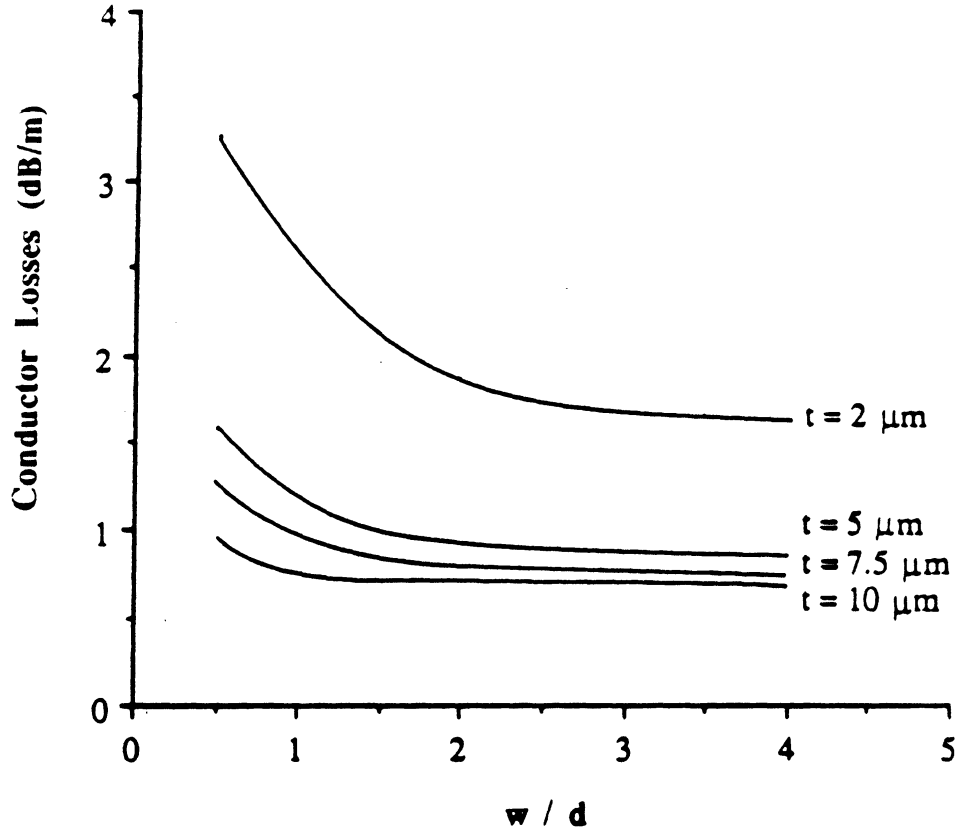

Figure 5: **Effect of Thickness on the Ohmic Attenuation Constant** (a = 10 mm, b = 20 mm, d = 1mm, ϵ_r = 10, σ = 3.33 x 10^7 S/m, f = 1 GHz)

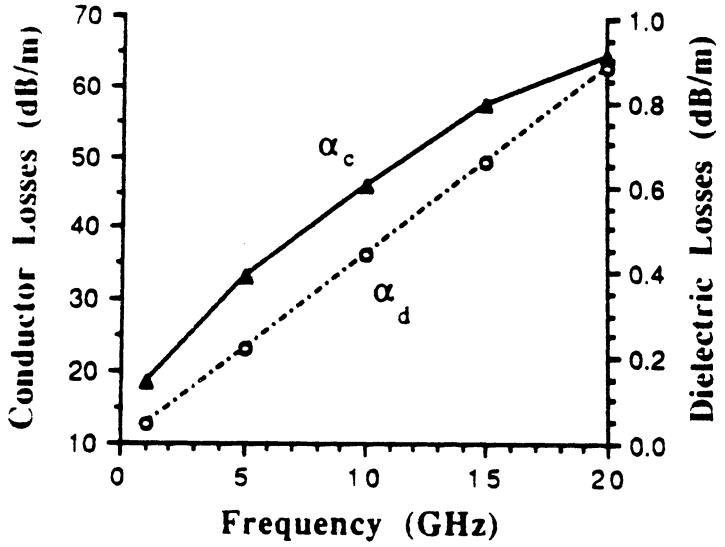

a. Dielectric and conductor losses vs frequency

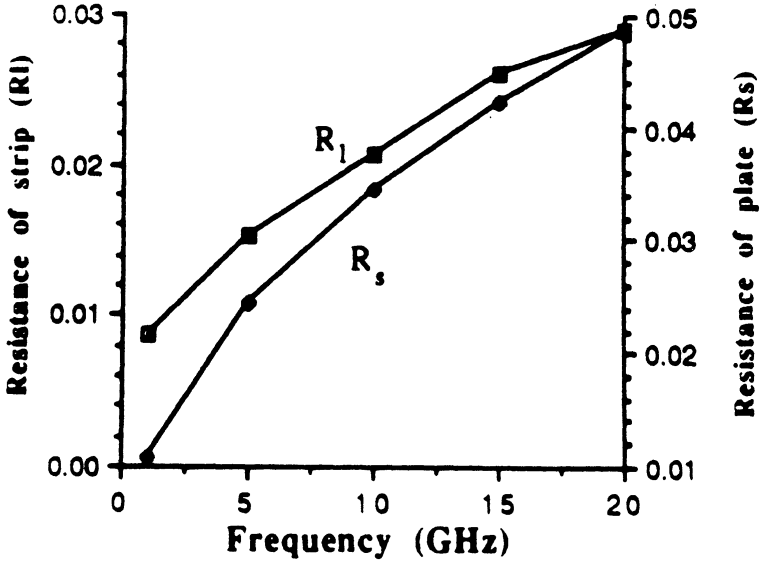

b. Equivalent surface resistivity R_l and ground resistivity R_s vs. frequency

Figure 6: Effect of Frequency on the Attenuation Constant ($a = b = 500\ \mu m$, $W = d = 50\ \mu m$, $\epsilon_r = 10$, $\sigma = 3.33 \times 10^7$ S/m, $t = 5\ \mu m$)

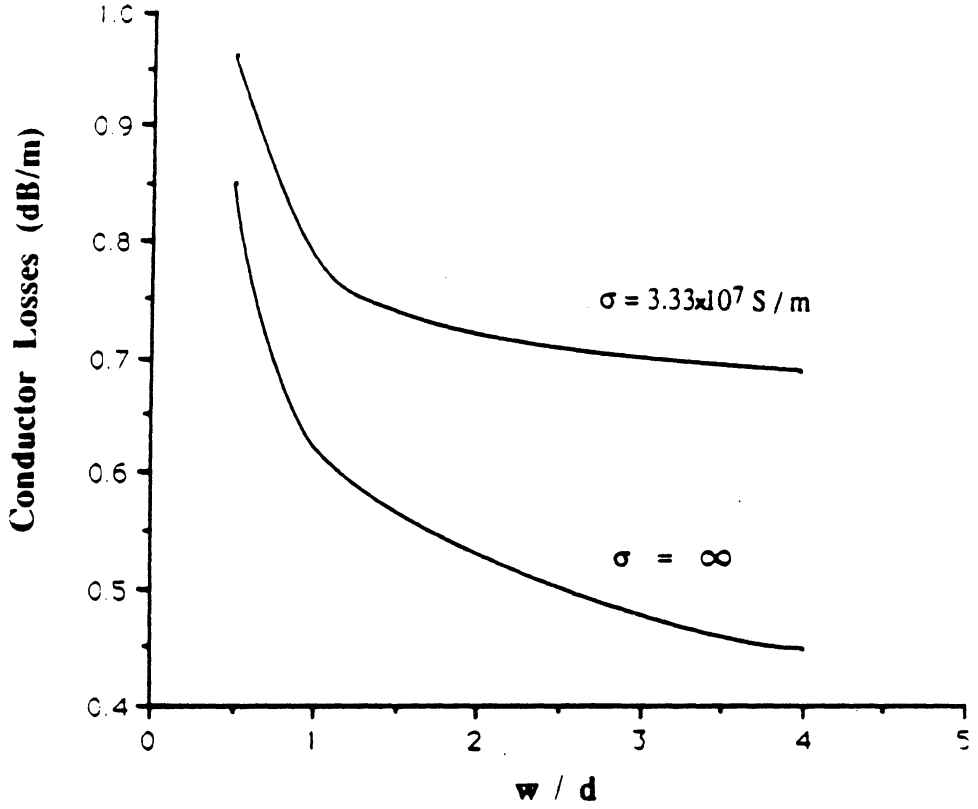

Figure 7: **Effect of Ground Plane Resistivity** on the Ohmic Attenuation Constant (a = 10 mm, b = 20 mm, d = 1mm, ϵ_r = 10, σ = 3.33 x 10^7 S/m, f = 1 GHz)

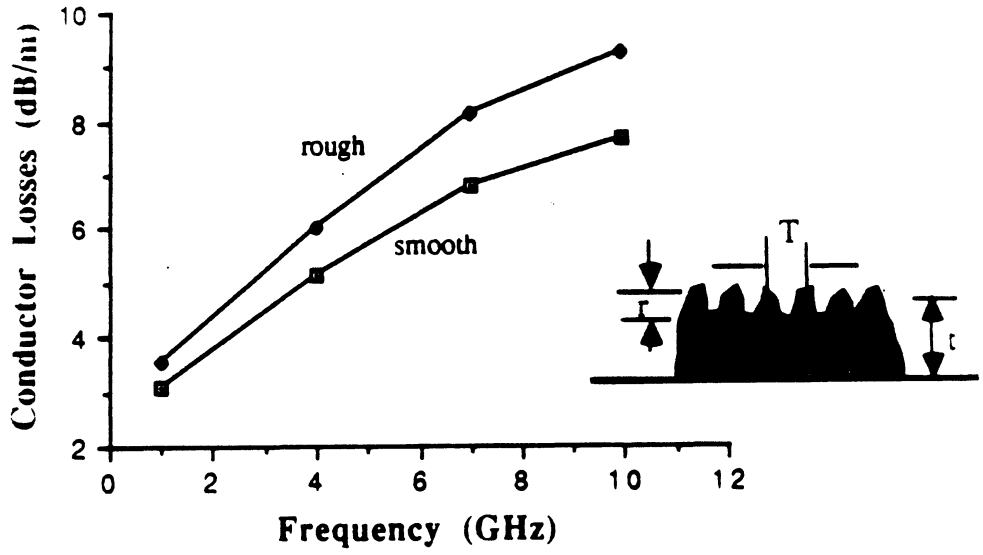

Figure 8: **Effect of roughness on the ohmic attenuation constant as a function of frequency** (a = 10 mm, b = 20 mm, $W = d$ = 280 μm, T = 70 μm, r = 1.5 μm, ϵ_r = 10, σ = 4 x 10^7 S/m, $t = 6\mu$m)

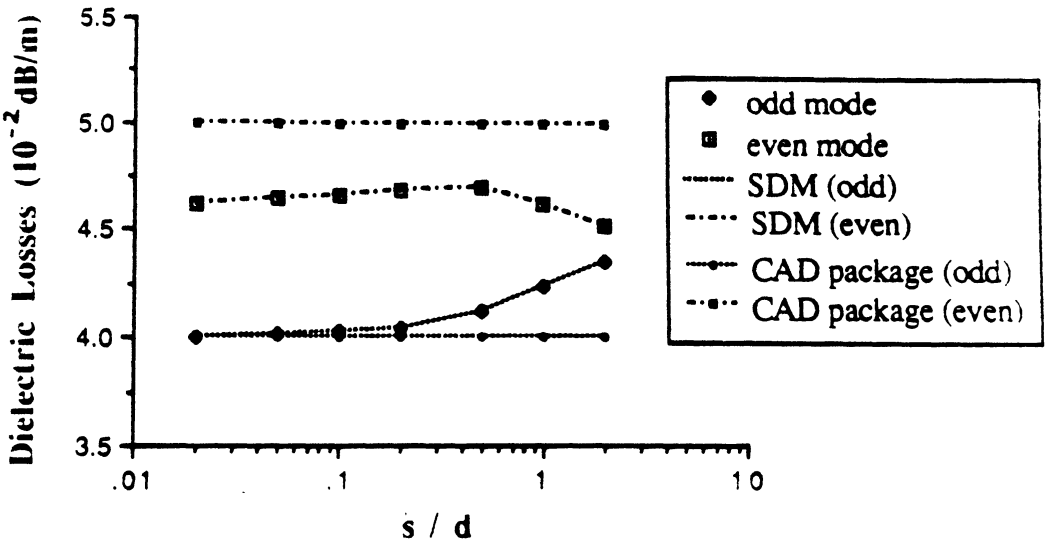

a. Dielectric attenuation as a function of s/d

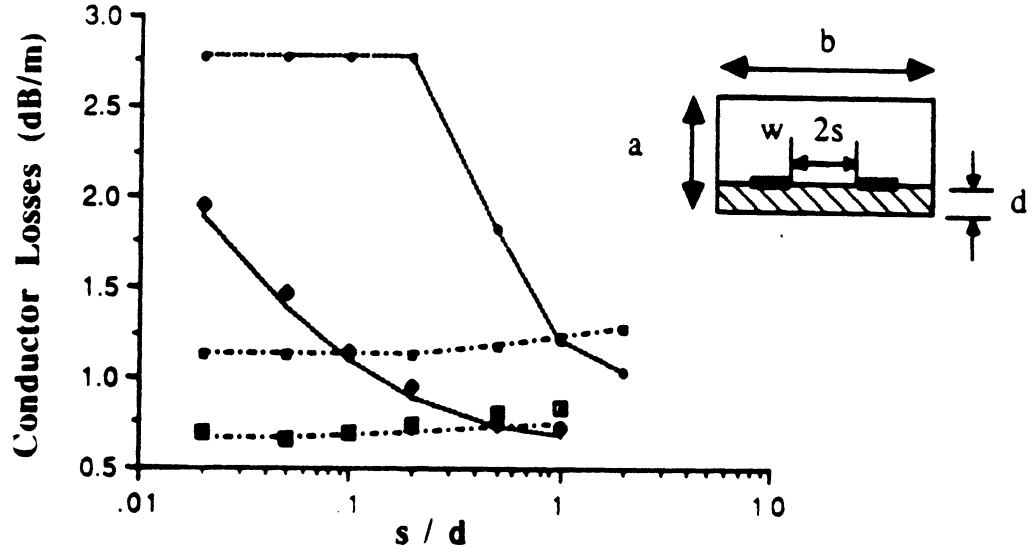

b. Ohmic attenuation as a function of s/d

Figure 9: Conductor and dielectric losses of coupled strips versus line separation (a = 10 mm, b = 20 mm, W/d =1, ϵ_r = 10, σ = 3.33 x 10^7 S/m, tanδ = 2 x 10^{-4}, f = 1 GHz, t = 0.01 mm)

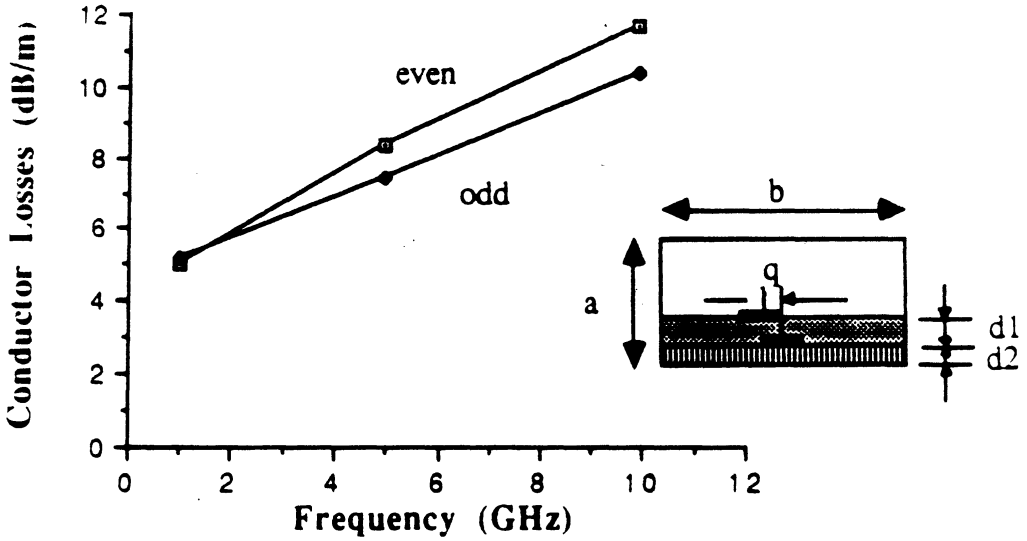

Figure 10: Ohmic losses of two-layer interconnects versus frequency (a = 1 mm, b = 2 mm, d_1 = 0.2 mm, d_2 = 0.1 mm, q = 0.5 mm, ϵ_{r1} = 4, ϵ_{r2} = 1, σ = 3.33 x 10^7 S/m, t = 4 μm)